UNIVERSITÀ DEGLI STUDI DI PADOVA

DIPARTIMENTO DI BIOLOGIA

Corso di Laurea magistrale in Molecular Biology

TESI DI LAUREA

The role of microglia-mediated neuroinflammation in a mouse model of perinatal stroke

Relatore: Aram Megighian, Department of Biomedical Science

Correlatore: Manuela Allegra, Neuroscience Institute, CNR

Laureando: Matteo D'Urso

ANNO ACCADEMICO 2023/2024

Table of contents

Abstract

Perinatal strokes, occurring during vital periods of brain development, can significantly disrupt neurological maturation. While the inflammatory response initiated by the stroke originates within the central nervous system, there is compelling evidence that an extensive peripheral inflammatory reaction, both acute and chronic, plays a crucial role. This reaction is driven by key inflammatory mediators and has a direct impact on the outcomes of ischemic brain injuries. Microglia, the brain's resident immune cells, are central to the brain's response to injury and development. Upon activation by stroke, these cells contribute to the pathology while also participating in attempts to repair the brain. Recent findings emphasize the significance of inflammation as a risk factor for enduring neurodevelopmental impairments, though a thorough understanding of the dynamics between systemic inflammation, microglia activity, and behavioural consequences is still lacking. To explore this further, we induced cortical lesions in mouse pups at postnatal day 14 (P14) using middle cerebral artery occlusion (MCAO). We assessed motor functions through gridwalk test, examining both immediate and long-term effects. Peripheral blood samples were also analysed to identify correlations between systemic inflammation levels and individual behavioural outcomes. Furthermore, we explored the impact of microglia depletion using a 7-days treatment with the CSFR-1 inhibitor, PLX-5622, to better understand their role in the context of perinatal stroke.

Overall, we found that ischemic stroke induces long-lasting motor impairments in mice, thus validating an animal model for perinatal stroke. Moreover, I characterized the neuroinflammatory response after stroke opening new questions about microglia. The treatment used to rescue this phenotype exacerbates neuronal death, although further analysis will be needed to determine the role of microglia-induced neuroinflammation after a perinatal brain injury. Finally, stroked animals clustered based on their motor recovery presented a different cytokines profile during the acute phase post stroke, opening the possibility to the identification of novel prognostic biomarkers.

1. Introduction

1.1 Definition, epidemiology, incidence

Stroke is defined as the interruption of the blood supply into the cerebral vasculature. Stroke represents the second leading cause of death and disability with 143 million disability-adjusted life years lost (DALYs) worldwide, affecting 13.7 million people per year. The annual mortality rate of 5.5 million is further compounded by a high co-morbidity as up to 50% of the survivors are chronically disabled. It has estimated that there are more than 80 million of stroke survivors globally, this number is almost double in the last 30 years. This population represents a high-risk community and the target of prevention and rehabilitation strategies. Indeed, the outcomes of stroke are generally poor with hemiparetic cerebral palsy, epilepsy, motor, and cognitive disabilities, including memory and learning impairments, which last a lifetime[1].

Stroke prevalence is about 1 out of 1000 people has a stroke every year and the risk increase as function of age. Despite that, in 2019, 63% of stroke happened in people younger than 70 years old, highlighting that stroke is no more an elderly disease[2].

Moreover, beside the physical and emotional sufferance caused by stroke for both patients and dears, stroke remarkably impacts on worldwide economy. In 2019, the estimated global cost of stroke is over US$891 billion (1,12% of the global GDP), a further motivation to enhance preventions and improve treatment of stroke disease.

To note, as shown in Fig. 1, stroke incidence is function of the level of a country's income, with higher incidence in high-income countries. These differences could be due to dissimilarities in life expectancy, social status, country standards of health-care provision and demographic age.

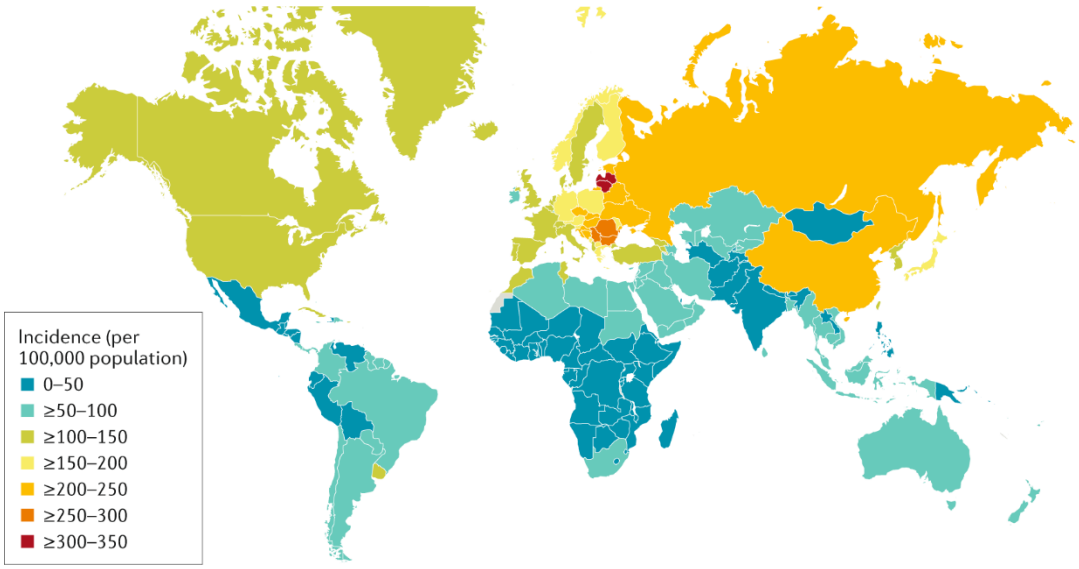

Figure 1. Worldwide distribution of stroke incidence by country. *Data from the Global Burden of Disease Study 2017.*

Based on the time of occurrence, stroke could be classified in perinatal, which include from 20 weeks of gestation up to 28 days of postnatal life, paediatric, up to 18 years of life, and adult stroke. Different ages in which the disease could emerge are associated with different outcomes. Moreover, the causes of the pathology and, consequently, the strategies of prevention, are distinct in function of age.

1.2 Risk factors

Non-modifiable uncontrollable risk factors for stroke are age, sex and genetic factors. Although stroke incidence increases with age, with a prevalence of 78% of people who experienced stroke above 50 years old, an increasing number of under 60 years old people who has experienced stroke during their life is remarkably increasing[2].

Sex is also associated with stroke disease, with a slightly higher incidence in men than in women, 133 versus 99 cases per 100.000 people per year in 2013 (2013 Global Burden of Disease Study).

Monogenic causes of ischaemic stroke have been identified, such as cerebral autosomal dominant arteriopathy with subcortical infarcts and leukoencephalopathy (CADASIL) and cerebral autosomal recessive arteriopathy

with subcortical infarcts and leukoencephalopathy (CARASIL), despite that most of the cases are sporadic[2].

Modifiable risk factors for ischaemic stroke include hypertension, absence or low levels of physical activity, a high apolipoprotein B (ApoB)-to-ApoA1 ratio, diet, a high waist-to-hip ratio, psychosocial stress and depression, smoking, cardiac causes, high alcohol consumption and diabetes mellitus[2]. These factors account for 91.5% of the population attributable risk of stroke worldwide.

Other potential risk factors include sleep apnoea, chronic inflammation, periodontal disease, chronic kidney disease[2]. Furthermore, several studies linked increased exposure to air pollution with transient increase in stroke incidence[2].

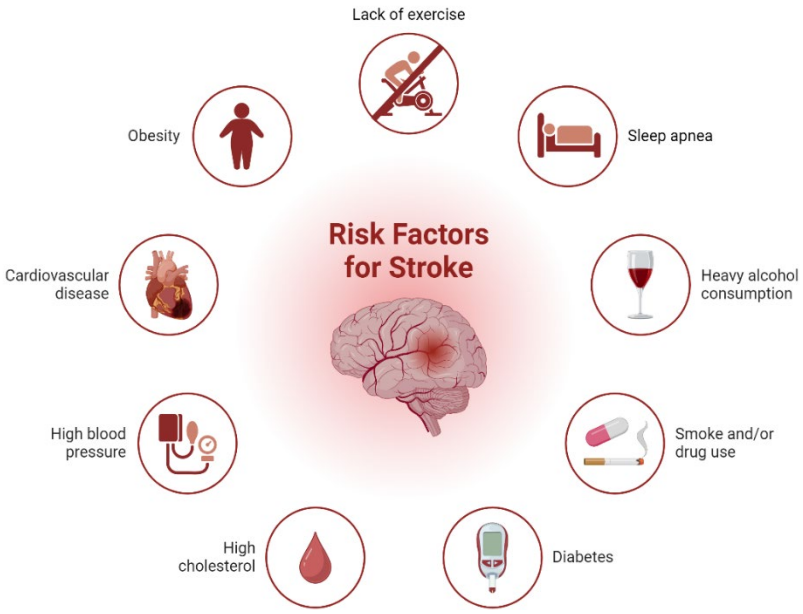

Figure 2. Non-modifiable risk factors accounting for the majority of stroke insurgency cases *(Biorender.com).*

1.3 Stroke Mechanisms and Pathophysiology

Based on its causes, stroke can be broadly classified into ischaemic and haemorrhagic, with the first one representing 85% of all strokes globally[3].

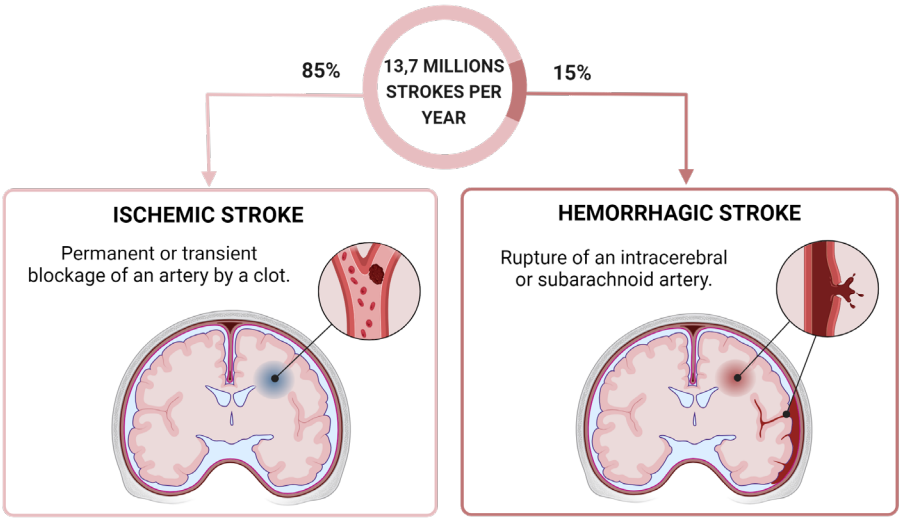

Figure 3. Stroke caused-based classification *(Biorender.com).*

Haemorrhagic stroke is caused by the rupture of a subarachnoid or intracerebral artery as results of traumatic events. The main types are intracranial stroke, when the bleeding occurs inside the brain, and subarachnoid, when the bleeding occurs between brain and meninges.

Ischaemic stroke is defined as infarction of the brain, spinal cord or retina and occurs when blood flow is transiently or permanently interrupted due to the presence of a clot into a cerebral artery. The global incidence and prevalence of ischaemic stroke are respectively decreased and increased between 1990 and 2013, as consequences of the improved prevention, detection and treatment of the pathology[4].

Ischaemic stroke mainly presents a thromboembolic origin, which common causes of embolism are atherosclerosis and cardiac diseases, in particular atrial fibrillation. Other basis of stroke are arterial dissection, vasculitis, patent foramen ovale (PFO), small vessel disease, diabetes mellitus and hypertension. The identification of the causes is fundamental to understand the molecular processes leading to the pathology guiding preventive and therapeutic strategies.

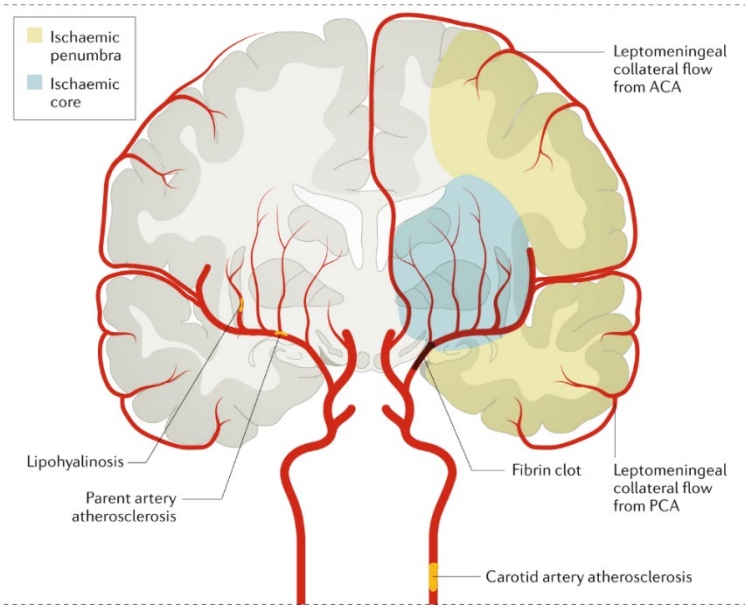

Figure 4. Ischaemic stroke mechanism *(adapted from Campbell et al., 2019).*

When an intracranial artery is occluded, alternative blood flow vessels, namely collaterals, can temporarily maintain the viability in the infarcted area. The extent of collaterals is interindividual dependent, presenting both genetic and environmental determinants. Moreover, collateral flow varies during life[2]. An important source of collaterals is the circle of Willis, however, it is often incomplete and the presence of downstream occlusion is common. Another more relevant source of collaterals is via leptomeningeal anastomoses.

Alternative blood flow pathways can be analysed by neuroimaging using CT, perfusion MRI and catheter angiography, identifying patients with good or poor collateral flow. Indeed, patients with good collateral flow represent the best candidate for reperfusion treatment approach even in delayed time window[5].

The pathophysiological processes following stroke occur in a time-dependent manner and can be subdivided into different functional stages of impairment and recovery. According to the species, different time windows can be identified and associated with different pathological processes. In humans, the hyperacute phase involves the first 24 hours following stroke, the acute phase is from day 1 to day 7, the early sub-acute is from day 7 to 3 months, the late sub-acute involves the period between 3 and 6 months, and the next and last phase occurs after 6 months from stroke and it is defined as chronic[6] (Fig. 5).

While, in mice, the injury progression after an ischemic stroke can be subdivided into three different stages: the acute phase (0-2 days), the sub-acute phase (2-30 days), and the chronic phase (from 30 days on)[6].

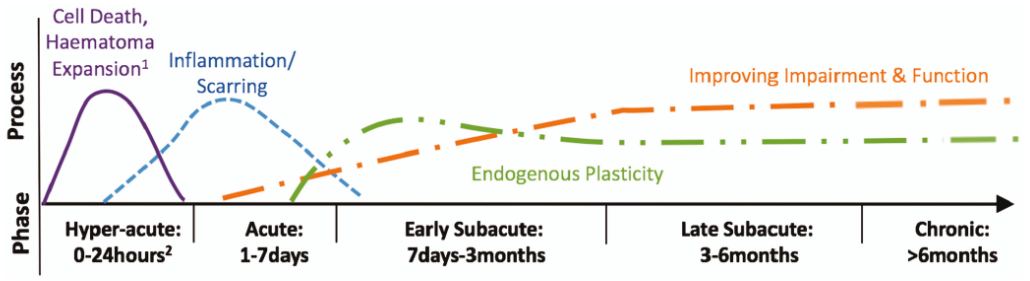

Figure 5. Framework of critical post-stroke time points that link to the currently known biology of recovery (*adapted from Bernhardt et al., 2017).*

1.3.1 Pathophysiology: impacts on neuronal cells and circuits

The main consequence following ischaemic stroke is the depletion of oxygen into the brain, leading to several detrimental cellular and molecular outcomes, affecting neuronal, glial and vascular tissues. In the 1970s, pioneering experiments demonstrated that the majority of the post-stroke deficits are caused by the hypoperfused, electrically-non-functional part of the brain, defined as ischaemic penumbra[2]. Such area is progressively and irreversibly converted into necrotic tissue, if hypoperfusion is maintained, and it is theatre of different kind of cell death events, among which apoptosis, necrosis and piroptosis, caused by the lack of oxygen and ATP. These events elicit a neuroinflammatory response that lead to the spreading of the aberrant non-homeostatic environment in the perilesional areas, determining the diffusion of the penumbra[7].

In addition, the energy deprivation prevents transmembrane gradient maintenance, determining the loss of the resting membrane potential. The main consequence of that is the anoxic depolarization at presynaptic terminals, which leads to neurotransmitter release[8]. This process is not counteracted by neurotransmitters' clearance that, indeed, is an active, energy-dependent process. For these reasons, neurotransmitters' concentrations increase during stroke in the ischaemic penumbra, enhancing the excitability of the injured areas and promoting aberrant electrical activities[9].

Moreover, the excitotoxic environment is particularly detrimental because of the presence of NMDA receptors in the post-synaptic terminals. At resting membrane potential, the electrical conductance of NMDA is almost null, thanks to the presence of an extracellular magnesium ion which works as a gate and blocks the channel pore. As a consequence of the extensive anoxic depolarization, NMDAr open aspecifically: this event, in fact, leads to the loss of the so called "Mg^{2+} block", triggering NMDA-mediated intracellular calcium influx. Calcium influx promotes calcium release from intracellular storages, triggering an exponential increase of its intracellular concentration. Calcium finely regulation of its intracellular concentration is well known to be essential in many processes underlying neurons activity[8]. Furthermore, several Ca^{2+}-dependent signalling pathways are thus activated, among them neuronal nitric oxide synthase activation, which lead to the production of free radicals. Additionally, nitric oxide (NO) works as retrograde neuromodulator, influencing synaptic transmission efficacy by triggering synaptic plasticity processes.

Globally, the random and aspecific activation of these processes in the context of pathology, may possibly contribute to abnormal forms of neuroplasticity which affects the neuronal local circuitry and whole network stream of information[2].

In point of fact, non-canonical electrical activity has been observed following brain injury; it is often initiated in the anoxic area but rapidly propagates to the surrounding, perilesional ones, increasing the energetic demand and may contributing to infarct expansion[2]. In addition, such abnormal neuronal activity has been observed in other pathological contexts, such as epilepsy, schizophrenia and psychosis[9]. Unfortunately, the meaning and role of this process is still not completely clear.

Other detrimental cellular effects following ischaemic stroke are neuronal ubiquitin depletion which leads to the accumulation and aggregation of oxidized proteins, causing endoplasmic reticulum stress. Mitochondria are also affected, in particular, several changes have been observed, among which protease activation, increased cisternal calcium levels, release of pro-apoptotic factors and free radicals, globally lowering energy production efficiency[2].

Several potentially therapeutic target pathways have been identified and treatments targeting them were demonstrated efficiently in animal models of ischaemic stroke. Despite that, the translation of these therapeutic approaches on humans led to unsuccessful results. The translation failure could be explained by different factors. First of all, there are substantial differences in brain structure, coagulation system and functional complexity between rodents and humans, leaving open the possibility that different pathological mechanisms could be involved in human disease compared to animal models (O'Collins et al., 2006).

1.3.2 Pathophysiology: impacts on glial cells

The central nervous system (CNS) parenchyma is compounded by many interacting cell types creating a complex environment, indeed, macroglia and microglia are essential for neuronal functionality. Astrocytes assists and feeds neurons, modulates synaptic transmission thanks to the expression of metabotropic receptors and the release of neurotransmitters, cleans the synaptic cleft from neurotransmitters, filters trophic factors, molecules and nutrients entering in the brain and monitors the neuronal environment[10].

Unlikely, macroglia and microglia cells are also affected by stroke. For example, stroke increases the activation of metabotropic glutamate receptor 5, increasing levels of intracellular calcium, which, in turn, leads to the internalization and reduction of the expression of glial glutamate transporters, affecting glutamate clearance[10]. Furthermore, astrocytes become reactive, acquiring pro-inflammatory (A1) or immunomodulatory (A2) phenotypes which are respectively protective and harmful. Reactive astrogliosis typically characterize the first 48-96h after stroke occurrence, leading to the generation of glial scar in the proximity of the injury which inhibit neuronal restoring[10].

Oligodendrocytes support neurons in the CNS by the generation of myelin sheaths which wrap their axons, with a single oligodendrocyte contacting more than 50 neurons' axons. Myelinization enhanced the electrical isolation of the axonal membrane, increasing the distance the electrical signal can travel before its decay. Myelinization is the evolutionary strategy adopted by higher organisms to sustain high-speed long-range electrical communication. The effects of stroke on

oligodendrocytes are not well investigated as the ones of astrocytes, despite that, it is known that oligodendrocyte and their progenitors tend to decrease in the ischaemic core through processes of cellular death. This process results in a transient demyelination affecting neuronal communication. Parallel, the two weeks after stroke are characterized by an expansion of oligodendrocytes, resulting in remyelination of the peri-infarcted area[10]. Furthermore, several studies showed that the expression of Nogo-A protein, an important inhibitor of synaptic plasticity *via* axonal remodelling, is increased in both the ipsilesional and controlesional cortical areas following middle cerebral artery occlusion (MCAO). Nogo-A is expressed by oligodendrocytes, excitatory pyramidal neurons and parvalbumin expressing inhibitory interneurons. The enhanced expression of Nogo-A was revealed detrimental, inhibiting beneficial processes of circuitry remodelling after ischaemic stroke. Thus, targeting Nogo-A with specific antibody represent a promising therapeutic target to promote neuronal reorganization and improve functional recovery after ischaemic insults[11].

Pericytes are spatially isolated contractile cells which constitute part of the blood brain barrier (BBB), controlling the cerebral blood flow. Their functions account for the filtering and regulation of compounds entering into the brain parenchyma, such as trophic factors, nutrients and endocrine molecules. After stroke, pericyte responses determine capillary constriction to limit blood flow and reduce the risk of haemorrhage. Pericytes cell death has been reported after ischaemic events, determining the rupture of the BBB and the consequent infiltration of peripheral immune cells into the brain parenchyma[12].

1.3.3 Neuroinflammation

In rodent models of stroke, early inflammation is mainly mediated by the activation of the resident CNS immune cells, microglia, which promote the release of molecules recalling and activating far microglia cells in a paracrine fashion. Later on, peripheral macrophages, lymphocytes and neutrophil migrate to the brain parenchyma, entering into the brain through the damaged BBB. Within the first 3 days after stroke, neutrophil accumulation has been observed preferentially in the ischaemic core, while reactive proliferating microglia localize in the ischaemic penumbra. The next stage sees the acquisition of an ameboid morphology and the

clearance of cellular debris by both microglia and peripheral macrophages. In particular, it has been demonstrated that macrophages acquire a pro-inflammatory phenotype during the acute phase after the brain insult, which is characterized by an intensive expression of NADPH oxidase, inducible nitric oxide synthase and major histocompatibility complex class 1 (MHC). At later stages (chronicization), macrophages go through a phenotypical transition to an anti-inflammatory identity, characterized by the expression of CD206 and CD163 receptors. Anti-inflammatory macrophages stop the secretion of pro-inflammatory cytokines, such as IL-1β, interferon-γ, IL-6 and TNF-α, and reduce phagocytosis, starting secretion of neurotrophic and protective factors[13].

Manipulating the inflammatory response can be a target to develop new treatment strategies, despite that, so far, its therapeutic potential is still unclear. Treatment targeting the Il-1 receptor or the α4 integrin (CD49a) signalling showed protective effect on animal models. Although that, phase I and phase II clinical trials on humans led to discordant results[14]. Further studies are necessary to elucidate the impact of modulating inflammation on functional recovery.

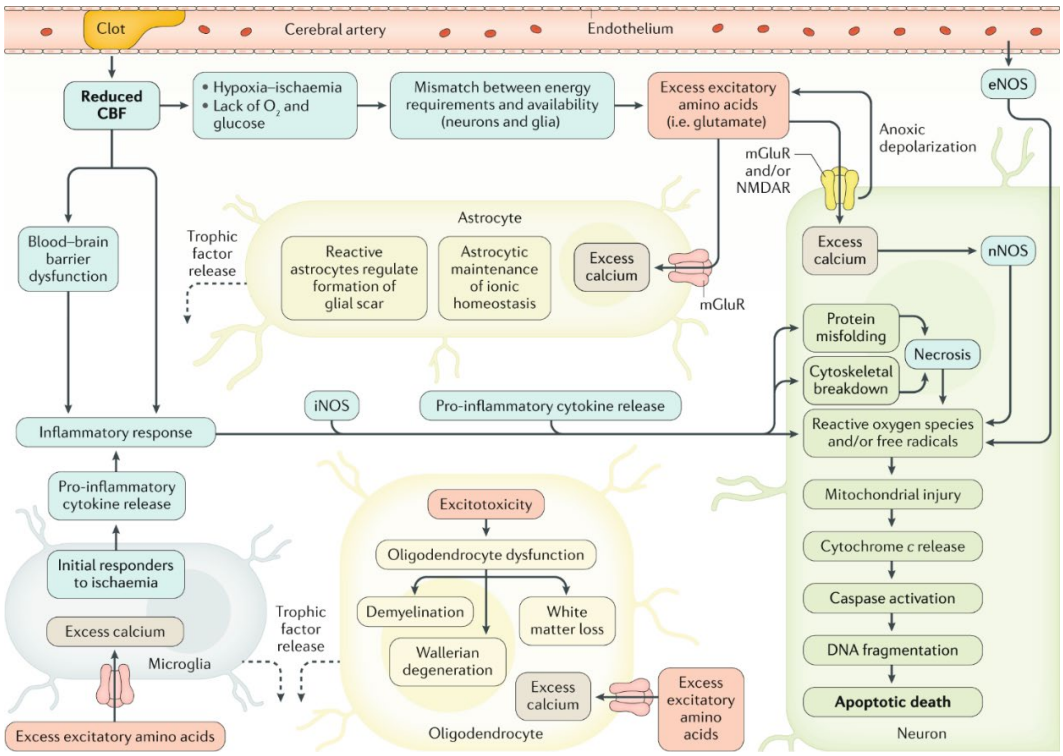

Figure 6. Ischaemia cellular cascade *(adapted from Campbell et al., 2019).*

1.3.4 Systemic effects

The subsequent consequences to a large ischaemic stroke include hypertension, arrhythmias, bradycardia, and pulmonary exudates[15], but if these co-morbidities are the direct result or a secondary effect of the brain insult is not clear. For example, cardiac alternations derived by severe brain injury could contribute to a reduction of the efficient perfusion of the initially unaffected or partially affected brain regions by the original insult, inducing a worsening of the outcomes. Furthermore, even focal restricted strokes can induce systemic responses, such as macrophages and stem cells release from the spleen and the bone marrow respectively, immune response, stress response and changes in gut permeability and microbiota[13].

Despite the majority of these systemic responses are beneficial for the recovery and represent an adaptation to restore the homeostasis, their chronicization is detrimental and partially accounts for the co-morbidities insurgency after stroke. Thus, the systemic responses to stroke are a potential therapeutic target.

1.3.5 Mechanisms of innate recovery

The extent of functional recovery in animal models of stroke is noteworthy, and similar ameliorations have been observed in young patients following stroke or traumatic brain injury. The main cause of this recovery is neuroplasticity, which allows remodelling of the neuronal connectome via alternative pathways which partially restores the lost functions. The main underlying processes, accounting for the neuroplasticity, are local sprouting, synaptogenesis, synaptic transmission plasticity. To note, several studies suggest that this neuroplasticity presents a cost. In particular, patients presenting a good recovery are often characterized also by difficulties to follow simultaneous events and fatigue[2]. This was assessed by imaging studies which elucidated that, in this condition, to reach normal function is necessary the recruitment of a higher proportion of neuronal circuitry, increasing the effort[16].

Endogenous stem cell contribution has been suggested by their detection in animal models and humans in the peri-infarcted area. These cells may contribute to the restoring of the neuronal environment promoting neurogenesis and neuroplasticity through the production of trophic and supportive factors[17]. Accordingly, exogenous

stem cells introduction may represent an interesting field for treatment development.

1.4 Diagnosis, Screening and Prevention

The diagnosis of stroke is initially based on symptoms including migraine, seizures, vestibular disturbances, metabolic disturbances, aphasia, hemiparesis, hemianesthesia, homonymous hemianopia, hemispatial inattention, and it is then confirmed by neuroimaging. Non-contrast computed tomography (CT) and magnetic resonance imaging (MRI) are the first-line imaging modality to diagnose stroke. The main limitations are the absence of rapid access to MRI in minority centres worldwide and that some patients are unable to have an MRI due to metallic implants or anxiety.

Moreover, neuroimaging allows to test the suitability of thrombolysis or thrombectomy in different patients and the salvageable tissue which are likely to benefit from reperfusion[2].

Non-contrast CT of the brain has close to 100% sensibility for the detection of intraparenchymal and extra-axial haemorrhage, being the election technique for the thrombolysis treatment decision making. Stroke diagnosis is also highlighted by early ischaemic changes, such as loss of grey matter and white matter differentiation, representing oedema or hyperdense arteries. However, these signs are uncommonly observable in the early phase after stroke[2].

MRI offers multiple configuration that evaluate distinct functional and structural characteristics of brain tissue, among which perfusion MRI, diffusion MRI and T2-based MRI. Diffusion MRI asses the dynamics of water molecules, diffusion become abnormal within few minutes after ischaemic stroke and it is restricted to regions of cytotoxic oedema, where there is an abnormal distribution of water molecules between intracellular and extracellular environment. It is the most sensitive technique to detect ischemia[2].

1.5 Treatments, Recovery and Rehabilitation

Antiplatelet therapies are low-cost and widely applicable treatments during the first 48h after the brain insult, reducing the occurrence of recurrent ischaemic stroke and improves outcome. Apirin-dypiridamole or clopidogrel are given acutely and continued for 3 weeks after stroke reducing the incidence of secondary stroke events in patients at high risk[2].

Currently, the most diffused and efficient reperfusion therapies applied to treat ischaemic stroke are intravenous thrombolysis and endovascular thrombectomy, despite they are both time-critical and subject-specific effectiveness[18].

There are two main drugs widely used for intravenous thrombolysis: alteplase and tenecteplase. The former one is a modified form of tissue plasminogen activator (tPA), leading to the cleavage of plasminogen into plasmin, which, in turn, degrades fibrin and dissolves the thrombus. The therapy is then followed by 1h infusion. The optimal time of intervention was set by many clinical trials, from which emerged that the greater clinical benefits are obtained administering the drug up to 4.5h after the symptom's onset. The ameliorative effects regard the reduction of the penumbra extension. It has to be taken into account that the thrombus lysis susceptibility decreases over time[18].

Tenecteplase is a genetically modified tPA with a longer life-time, greater resistance to inhibitor and fibrin specificity. Several studies highlight an enhanced efficacy and safety of tenecteplase compared to alteplase. Despite that, tenecteplase is now licensed only in India to treat ischaemic stroke[2].

The main adverse off-side effect of thrombolysis is haemorrhage, which can worsen the cerebral damage. Based on that, beside the time span of administration, it is fundamental to take into account risk factors that increase the probability of systemic or intracerebral haemorrhages. Among these factors: hypertension, recent trauma or surgery, the use of anticoagulants or coagulopathies and recent intracerebral haemorrhage[19].

Endovascular thrombectomy (EVT) is a minimally invasive surgical procedure which aims to the removal of a blood clot from an obstructed artery in the brain, restoring the normal blood flow. The procedure exploits a catheter which is inserted

into the artery, once it is placed, a stent retriever is used to eliminate the blood clot. The major risk for this procedure is haemorrhagic stroke transformation, which could be caused by arterial perforation or dissection. Despite that, these collateral effects are very uncommon, less than 1.3%, as reported in the study of Campbell and colleagues, 2018[20]. In addition, EVT is a valid and safer alternative for patient's ineligible for intravenous thrombolysis.

Many clinical trials of rehabilitation strategies have been performed after ischaemic stroke, unlikely all these attempts were neutral or harmful. An additional layer of complexity derived from the interpretation of the efficacy of the intervention, indeed, the discrimination between the intrinsic recovery and the benefits due to the rehabilitation is very problematic (AVERT Trial Collaboration Group, 2015).

In conclusion, the absence of long-lasting impairments treatments shows up the necessity to improve the knowledge of stroke pathophysiology to develop new strategies aimed to ameliorate the functional recovery.

1.6 Perinatal stroke: definition, incidence and risk factors

Based on the time of occurrence, stroke could be classified in perinatal, which include from 20 weeks of gestation up to 28 days of postnatal life, paediatric, up to 18 years of life, and adult stroke. Different ages in which the disease could emerge are associated with different outcomes. Moreover, the causes of the pathology and, consequently, the strategies of prevention, are distinct in function of age.

Developmental stroke, including perinatal and paediatric stroke, represents sporadic cerebrovascular disorder and the main cause of hemiplegia in children[21]. More specifically, perinatal stroke account for approximately 25% of developmental stroke cases. Moreover, perinatal stroke incidence is between 1:1600 and 1:3000 live birth, presenting an approximately 70% ischaemic prevalence[21]. Unfortunately, the disease is often undiagnosed, influencing the real value of perinatal stroke incidence[21].

The developmental processes occurring during the perinatal period are species-specific. Consequently, the stroke impact on specific developmental processes involves different ages in different species. Based on that, it is fundamental to correlate neurodevelopmental stages of different organisms to be able to translate

the knowledge acquired from animal models to humans. As shown in Fig. 7, similar neurodevelopmental processes occur in different time windows during the perinatal stage in humans and mice.

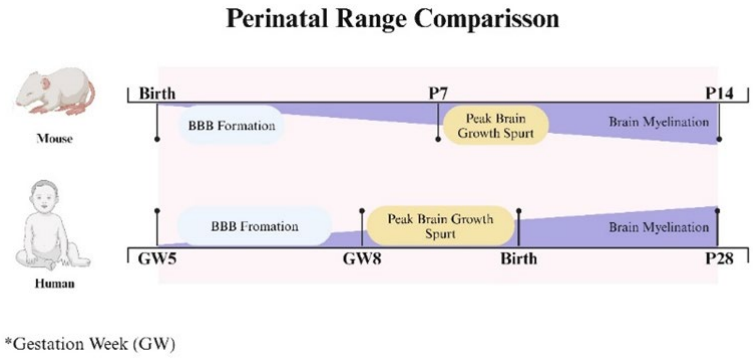

Figure 7. Comparison between the perinatal period in mice and humans *(Biorender.com).*

In 2021, Heléne E.K. Sundelin[22] and colleagues have investigated 1606 cases of developmental (perinatal and paediatric) ischaemic stroke, observing a mortality rate in the first 6 months of 40.1 per 1000 person-year. The overall mortality rate, indicated as hazard ratio (HR), was very high and remain elevated for 20 years after the injury. Furthermore, the insurgency of co-morbidities is remarkably enhanced after stroke, in particular stroke determines a higher risk of develop neurological, cardiac, endocrine, nutritional and metabolic diseases, and cancers. These results highlight how developmental stroke promotes long-term mortality and co-morbidities occurrence, influencing the entire lifetime of the affected individuals[22].

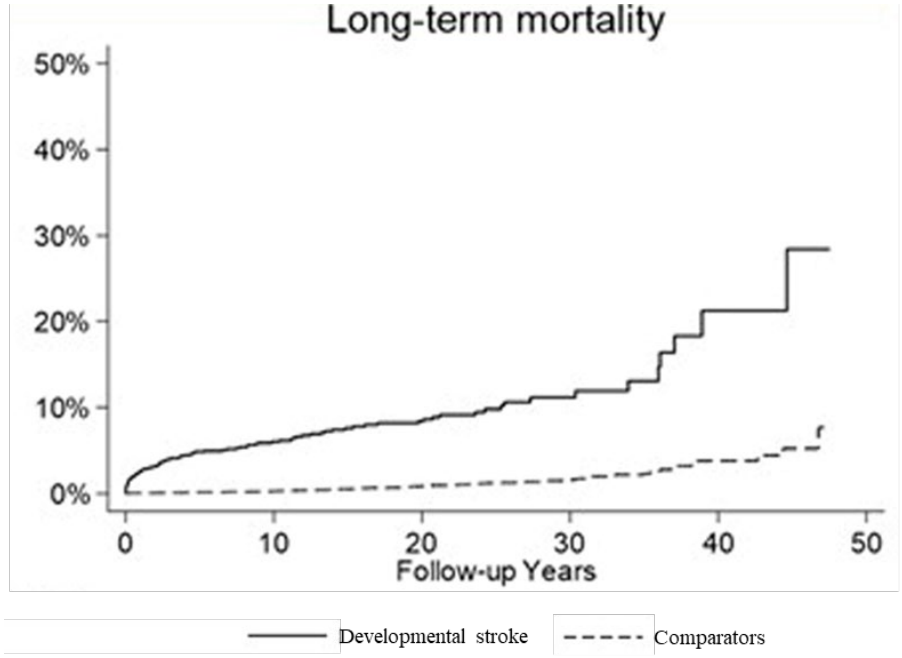

Figure 8. Long-term mortality after developmental stroke *(adapted from Heléne E.K. Sundelin et al. 2021).*

The importance of deepening the knowledge about developmental ischaemic stroke is evident comparing the efforts of the scientific community on study adult or perinatal forms of ischaemic stroke. Indeed, the number of studies focusing on adult stroke in the last ten years are more than 100 times more than the ones on perinatal stroke, highlighting how much is fundamental to improve the understanding of the pathophysiology of this tremendous developmental pathology in order to ameliorate the condition of the affected individuals.

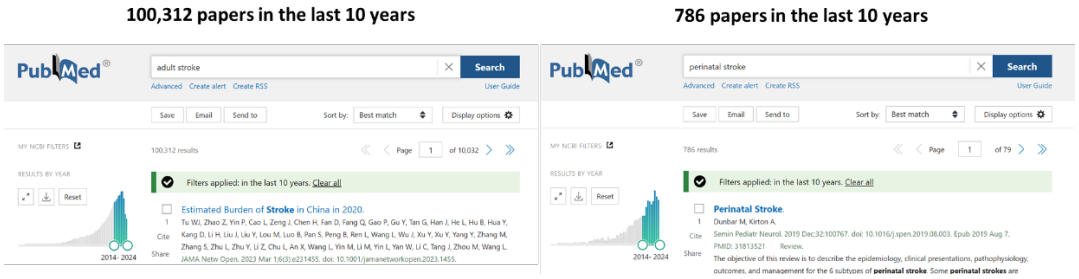

Figure 9. Comparison between the number of publications focusing on adult (left) and perinatal (right) stroke.

Specific risk factors for perinatal stroke include intrapartum fever, tight nuchal cord, emergency caesarean section, passing through fetal distress, pre-eclampsia, hypoglycaemia, small size for gestational age[21].

The consequences after perinatal stroke are mainly related to neurological impairments that affect cognitive, sensory, speech, and motor functionality. Therefore, the most common approach to improve the development outcome is the early motor-target intervention[21].

1.7 Microglia: origin, phenotypes and functions

The term "microglia" was presented for the first time in 1919 by Pio del Rio-Hortega, to define the population of resident CNS cells morphologically discriminable from macroglia cells, astrocytes and oligodendrocytes.

Microglia cells are tissue macrophages and constitute the innate resident immune system of the CNS[23]. Although closely correlated to circulating monocytes, microglia are morphologically and phenotypically different from other populations of mononuclear phagocytes within the CNS such as perivascular macrophages, supraependymal macrophages, epiplexus cells, and meningeal macrophages[23]. The absence of a precise lineage restricted marker for microglia progenitors is a key issue for the determination of the origin and lineage of these cells.

Microglia's origin is still a matter of debate, and different hypothesis have been formulated. The neuroectodermal hypothesis states that microglia present the same embryonal origin as neurons and macroglia[23]. To investigate this hypothesis, in 2003, Levison et al. isolated and cultured rats dorsoventral subventricular zone (SVZDL) embryonic progenitors and perinatal SVZDL neuronal stem cells to assess their potency to originate both microglia and macroglia. Neuronal isolated stem cells produced homogeneous and heterogeneous populations of macroglia but not microglia, supporting a different non-neuronal origin of microglia.

The mesodermal hypothesis supports the yolk-sac derivation of microglia's progenitors, which during embryonic and foetal periods migrate and colonize the developing CNS parenchyma before the constitution of the blood brain barrier (BBB)[23]. However, the processes controlling their migration and establishment are still poor understood. The main evidence supporting this theory derives from the work of S. Vitry and colleagues, in 2003,[24] which demonstrated the neuropoietic potential of hematopoietic precursors intraventricularly grafted into the brain. These multipotent cells gave rise to microglia in mice.

However, Ginhoux and colleagues, in 2010,[25] showed the practically null contribution to microglia homeostasis of homoeotic progenitors in the adult mice. By *in vivo* lineage tracing, it was demonstrated that adult microglia derived from primitive myeloid progenitors that arise before embryonic day 8, suggesting an ontogenically distinct identity of microglia cells among the mononuclear phagocyte system. Microglia turnover in the adult brain is a controversial topic, such as the source of these cells is difficult to determine. The main allowable hypothesis regards the self-renewal capacities of microglia *via in situ* proliferation, the replenishing from circulating blood and bone marrow precursors *versus* the existence of CNS progenitor's niches[23]. All these theories are sustained by many evidence, likely suggesting a coexistence of these different processes.

1.8.1 Phenotypes and functions

Microglia cells are very plastic and present a remarkable variability which is associated with different functions, signals in the brain and exposure of membrane-bounded secreted proteins[26]. Recently, one of the most diffuse techniques to study microglia is immunohistochemistry by which neuroinflammation and microglia reactivity can be qualitatively and quantitatively investigated. Despite microglia morphology is not fully indicative of microglia function, morphological outcomes are very useful to make inferences.

During development in mice, microglia colonize neuronal tissues at embryonic day 7.5-8 and rapidly proliferate. In this period, microglia present a preferentially ameboid phenotype which is functional for migration and invasion of the central nervous system. Flattened microglia have been observed along walls of blood vessels. In postnatal weeks 2-4, microglia increase size and present a higher degree of branching. This ramified morphology is essential during brain development, assisting synaptogenesis, monitoring brain environment and actively shaping the neuronal connectome by synaptic pruning[23].

In homeostatic conditions, microglia typically have a small soma and present a ramified morphology of the branches that allow monitoring of large volumes of the neuronal parenchyma[23].

When microglia detect a pathological stimulus, they acquire reactive phenotype, retracting their branches and enlarging the soma; this morphology, defined as ameboid phenotype enhance the efficiency of migration to the site of damage and the phagocytic potential[23].

Microglia reactivity is not an all or nothing process, intermediate microglia states have been observed between the two ameboid and ramified extremities. For example, bushed microglia with a large cell body and short, thick branches is known.

Furthermore, hyper-ramified microglia have been associated to pro-inflammatory conditions in many pathological conditions, such as in PTSD rats[27]. Other disease-associated microglia morphology are: rod microglia, whose role and functions is currently not clear, and dystrophic microglia which presents a fragmented shape and are abundant in neurodegenerative diseases and increase during aging. It has been proposed that this latter type of microglia represents a form of protective mechanism in which microglia assume a senescent phenotype. This hypothesis is supported by the positivity of microglia for multiple senescent marker[23].

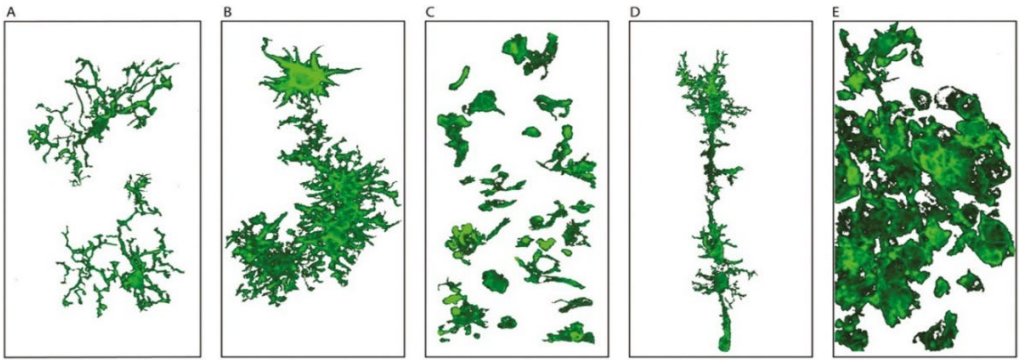

Figure 10. Microglial morphologies. *The images show different microglial morphologies adapted from photomicrographs of Iba1-stained cells. (A) Ramified microglia. (B) Bushy or hypertrophic microglia. (C) Ameboid microglia. (D) Rod microglia. (E) Microglial scar (adapted from Tabitha R F Green et al., 2024).*

1.8.2 Endogenous factors affecting microglia

Many endogenous factors influence microglia function. For example, it has been shown that sex could influence microglia in rodents; in particular, while male rats present a higher number of reactive microglia during early development, female rats have more reactive microglia during late development. Despite the meaning of this sex-based difference is not well understood, these evidence highlight how microglia could be affected by sex-specific and developmental processes[23].

Sex differences have been observed also in pathological context. After neonatal ischemia, male mice present a higher proportion of ameboid reactive microglia, suggesting an enhanced inflammatory response than female mice. In contrast, in adult mice, sham females show a greater number of microglia compared to sham males but no differences in terms of morphology have been observed. Moreover, liposaccharide administration affects microglia morphology in male mice but not in females. These contrasting results suggest that microglia can be affected based on the time of occurrence of the stimulus and the type of inflammatory insult[23].

Finally, the circadian rhythm and sleep work as regulators of microglia morphology. In particular, during sleep microglial morphology is more complex and ramified than during wake periods. This could be explained by the fact that during sleep microglia actively participate to restore the homeostasis conditions lost during the intensively active awake period. Moreover, circadian gene expression fluctuations reflect daily microglia morphology fluctuations, suggesting that microglia are affected by endogenous intrinsic cellular circadian rhythms[23].

1.9 The role of microglia in neuroinflammation after stroke

Microglia activation following ischaemic stroke plays a fundamental role in the body response to the insults. However, whether the meaning of microglia contribution is beneficial or detrimental depends on the diseases, the age of the individuals and time from the pathological event.

A common feature of stroke outcomes is that it promotes an inflammatory response. Microglia activation occurs early after the injury and can last for years after the damage[31]. The activation regions often coincide with the ones subjected to neuronal

degeneration and axonal abnormalities, although, it has been observed microglia activation can occur in far remote sites from the ones of focal injuries[28].

Microglia, as macrophages, chemotactically migrate in the injured area, in order to establish a protective environment to counteract the pathophysiological processes following the stroke[31]. With the aim to restore the loss homeostasis, during the acute phase, the main role of microglia is to eliminate cellular apoptotic and necrotic debris, which is accounted by the acquisition of an ameboid reactive morphology.

Dying cells release molecules which belong to the family of Danger-associated molecular patterns (DAMPs), which are perceived by the set of surface receptors expressed by microglia, in particular Toll-like 2 and 4, and Nod-like receptors (TLRs and NLRs). DAMPs perception triggers intracellular signalling pathways which converge on gene expression regulation[10].

At this point, reactive microglia release noxious substances, such as pro-inflammatory cytokines (e. g. IL-1β, IL-6), nitrogen species, reactive oxygen species (ROS) and, even, excitatory neurotransmitters as glutamate, which exacerbates the excitotoxic stroke-induced environment. Furthermore, the abundant secretion of pro-inflammatory cytokines can interfere with glutamate buffering activity of astrocytes, inhibiting the glutamate transporter and worsening the neurotoxic environment[10].

Therefore, endocrine, and paracrine microglia-mediated signalling recall and active resident and peripheral innate immune cells in the site of injury, exponentially enhancing the brain response to the damage. Based on the stage of the disease and the chronicity, microglia are differently stimulated, leading to the acquisition of different phenotypes which present distinct function, morphology and gene expressions. Microglia are primed by pro-inflammatory, such as IFN-γ, IL-1α, IL-6, and TNF-α, and anti-inflammatory cytokines which respectively lead to pro-inflammatory M1 and anti-inflammatory M2 phenotypes[28].

M1 phenotype promotes the secretion of pro-inflammatory factors exacerbating the brain injury, while M2 phenotype promotes the release of neurotrophic factors, promoting repairs, healing and neurogenesis, and parallelly inhibiting pro-inflammatory activities. The current view is that during the acute phase after stroke,

M1 microglia could play a beneficial role, allowing the clearance and restoring of the brain extracellular microenvironment, while the inflammatory chronicization lead to a worsening of the neurological manifestations. However, transcriptomic analysis has revealed that microglia display a highly dynamic phenotypic continuum than only M1 and M2, including mixed activation states[28]. This increases the complexity of investigating microglia involvement in pathology.

To conclude, the double-edge sword represented by microglia activity after stroke remarkably complicates the investigation of the role and involvement of microglia in the following pathological process after the insult. All these evidence highlight the importance of getting insight into the mechanisms of microglia involvement during the brain response after damage to elucidate its role in pathology. In particular, the modulation of microglia activity, with a particular focus on the time and the mechanisms of intervention, can be exploited as therapeutic targets to improve functional recovery[28].

1.10 Plexxikon (PLX) 5622

Plexxikon (PLX) 5622 is pyrrolopyridine, it derives from vemurafenib, an inhibitor of B-Raf and other kinases, intensively used antineoplastic agent. PLX presents the same structure of vemurafenib but with the p-chlorophenyl group substituted by chlorine. PLX, with a molecular formula of C17H14ClF2N3O3S and a molecular weight of 413.8 g/mol, is intensively used as antineoplastic and immunosuppressor agent. Furthermore, PLX is a specific inhibitor of the colony stimulating factor receptors (CSFRs), a family of survival receptors expressed by many cell types belonging to the innate immune system, such monocytes, peripheral macrophages and microglia. Indeed, PLX treatment induces a transient immunodeficiency by depleting CSFR-expressing immune cells, allowing to finely modulate the immune response after triggering insults[29].

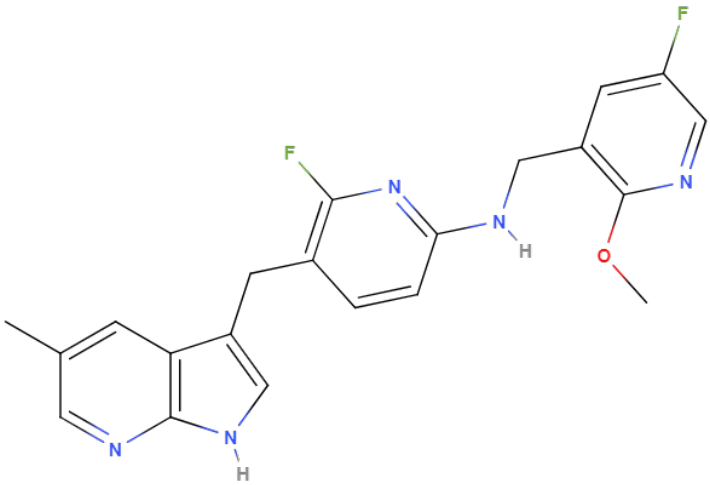

Figure 11. Plexxicon 5622 chemical structure.

1.11 Aim of the thesis

The main focus of my thesis work was to characterize the role of microglia-mediated neuroinflammation in a mouse model of perinatal stroke.

The project was designed based on a series of interlocked aims, and developed around two main objectives:

1. The validation of a mouse model of perinatal ischaemic stroke.

2. The characterization of the neuroinflammation induced after the ischemic stroke, through the modulation of the microglia activation.

First of all, the validation of dMCAO procedure to induce stroke will be obtained by assessing the anatomical consequences of the procedure. This validation is essential to correlate the behavioural outcomes with the ischaemic stroke modelling. After that, I aimed to evaluate the motor and cognitive impacts on the animal behaviour to determine if and which brain functions are affected by the dMCAO model.

The second part of my work was study how to manipulate microglia, which, as previously discussed, play a fundamental role but it was not always elucidated in stroke outcomes. The hypothesis of the project is that a reduction of the neuroinflammatory response after ischaemic stroke may enhance neuronal survival and promote the functional recovery. To test this hypothesis, I temporally depleted

microglia for a week after stroke induction to avoid the intense inflammatory response and consequent associated brain damages.

I then evaluated the cellular consequences of microglia ablation, among which neuronal loss, microglia phenotypes transitions and astrogliosis. Moreover, I also evaluated the impacts on functional recovery of microglia ablation through different behavioural tests evaluating motor and cognitive performances.

Finally, with the aim to discover diagnostic and prognostic biomarker useful for the development of individual-specific treatment, I subdivided stroked animals in good and poor recoverers based on the asymmetric motor impairments and then I evaluated their difference in terms of blood cytokines profiles.

2. Materials and Methods

2.1 Animals

In the following study, CD1 mice provided by Charles Rivers Laboratory were used. Two groups of eight mice each were divided into stroke and sham based on the surgery they received. Both males and females were used and randomly assigned to each experimental group. All mice were housed in the Institute of Paediatric Research (IRP) animal facilities with a 12 h light/dark cycle at an ambient temperature of 22°C. They were fed with standard pellet chow and reverse osmosis water. All experiments were performed according to the Italian ethics committee regulations, in accordance with the European directive on animal experimentation.

2.2 Surgical procedure: distal Middle cerebral artery occlusion (dMCAO)

The mice model of distal middle cerebral artery occlusion (dMCAO) was performed as previously established (Doyle Kristian P. & Buckwalter Marion S., 2014). The mice were randomly divided into two groups: the sham (control) and the stroke group (experimental). The stroke group were anesthetized in a chamber with isoflurane inhalation (2% isoflurane in 100% oxygen), once unresponsive, the skin of the right temple was shaved for the surgery. With a cotton swab fill with tincture of iodine the area was sterilized, an incision was done to expose and then remove the temporal muscle. Once the middle cerebral artery (MCA) was visible under the skull, with the help of scalpel, a craniotomy was performed to remove a rectangle of the skull and display the artery. The vessel was electro-coagulated with the electrocoagulation tweezers. After the procedure was complete and the occlusion was visually confirmed, the wound was close using surgical glue. During this whole process the animal temperature was maintained with the help of a heating blanket at around 37ºC. The sham group was treated under the same parameters with a sham surgery (Doyle et al., 2012).

2.3 Behavioural Testing

Fine motor impairments were assessed by grid-walk test, in which the mice is putted on a horizontal grid and recorded for 5' while it is walking. Mice were subjected to this test at day 2, 9 and very two weeks after stroke until the sacrifice. The videos were manually analysed by the same operator. The quantified parameters were the number of left and right forelimbs faults to compute the asymmetry index, a measure of the asymmetric motor impairments of the subject.

2.4 Blood Collection and Luminex assay

At the same time points of the behavioural tests, blood was collected from the submandibular vein of the animals with a sterile 21G nail. Importantly, blood collection has been performed after behavioural testing in order to avoid unnecessary stress possibly affecting mice performances Samples were subsequentially incubated in 1.5 ml Eppendorf with 10 µl of EDTA 0.5M, to avoid blood coagulation. The ratio between EDTA and blood has to be 1:10. Sample were then centrifugated at 1,500 x g (or 3000 rpm) for 10 minutes using a refrigerated centrifuge at 4°C to separate the corpuscular phase from the plasma. This latter one was then transferred into sterile polypropylene tubes (preferably 1.5 ml Eppendorf tubes) and stored at -80°C until it was analyses *via* Milliplex Mouse Cytokine/Chemokine MAGNETIC BEAD Premixed 32 Plex Kit.

In total 32 analytes (GM-CSF, Eotaxin (CXCL5), IFN-γ, IL-1α, IL-1β, IL-2, IL-3, IL-4, IL-5, IL-6, IL-7, IL-9, IL-10, IL-12p40, IL-12p70, LIF, IL-13, LIX (CCL11), IL-15, IL-17, IP-10, KC, MCP-1, MIP-1α, MIP-1β, M-CSF, MIP-2, MIG, RANTES, VEGF, TNF-α) were analysed by Luminex assay (Millipore, Billerica, USA) in the plasma from controls (sham) and 26 stroked mice. The diluted standard and quality control were used according to the manufacture's instruction. The plate was read on Luminex 200™. Analysis was performed using xPONENT 3.1 software.

2.5 Plexxikon 5622 treatment for microglia depletion

A stock solution of Plexxikon 5622 (PLX5622, HY-114153, MedChem Express) was prepared dissolving the powder in 10% dimethyl sulfoxide (DMSO, HY-Y0320, MedChem Express). The intraperitoneally (i.p.) injections from day 2 to

day 9 after stroke induction were performed at a final concentration of 65 mg/kg in sterile 0.9% NaCl and 20% Kolliphor40 (Sigma-Aldrich). Control mice received i.p. injections with the vehicle solution.

2.6 Tissue preparation

Animals were perfused at D23, D65 or D79 with an overdose of anaesthetic (ketamine 200 mg/kg, xylazine 50 mg/kg). Transcranial perfusions were performed using cold PBS followed by 4% paraformaldehyde (PFA; 441244, Sigma-Aldrich), pH 7.2–7.4, in PBS. The brains were then extracted, and post-fixed in 4% PFA overnight. Finally, brains were cut in a vibratome (VT1000S, Leica), and 60 µm thick coronal-slices were cryoprotected in antifreeze solution (50% 1x PBS, 20% glycerol (Sigma-Aldrich) and 30% ethylene glycol (Sigma-Aldrich), until mounting on single frosted microslides (2948-75x25, Corning).

2.7 Immunohistochemistry analysis

All the staining were performed in a 24 multi-well plate. The first step was to block the aspecific sites in the blocking solution (BS; 2% bovine serum albumin, 1% goat serum, 1% horse serum, in PBS-1X) with 0.5% Triton X-100 (648463, Sigma-Aldrich) for 1 hour at room temperature. Slices were then incubated with the primary antibodies in a 0.05% Triton X-100 BS solution, overnight at 4°C. Primary antibodies included rabbit anti-Iba1 (1:500; SAB5701363, Sigma-Aldrich), rat anti-CD68 (1:400; MCA1957, Bio Rad), chicken anti-GFP (1:400; AB5541, Merck) and rabbit anti-NeuN (1:400; EPR12764, Abcam). The next day, slices were washed 3x10’ with 0.01% Triton X-100 in PBS, followed by 2 hours of secondary-antibody incubation at room temperature. Secondary antibodies included goat anti-rabbit Alexa Fluor™ 568 (1:500; A-10042, Thermo-Fisher Scientific) to target Iba-1, donkey anti-rat Alexa Fluor 488 (1:400; A-21208, Thermo-Fisher Scientific) to target CD68, donkey anti-rabbit Alexa Fluor 488 (1:400; A-21206, Thermo-Fisher Scientific) to target NeuN and donkey anti-chicken Alexa Fluor 568 (1:400; A-78950, Thermo-Fisher Scientific) to target GFAP, dissolved in BS. Slides were washed 3×10’ in 0.01% Triton X-100 in PBS and incubated with HOECHST-33258 (1:1000; Cat: 40044; Sigma-Aldrich) dissolved in PBS for 6’ to label cell nuclei. Finally, slices were mounted on single frosted microslides with Vectashield® Plus

Antifade Mounting Medium (Cat: H-1900; Vector Laboratories), coverslipped and stored at 4 °C until imaging.

2.8 Fluorescent microscopy

Coronal brain slices of 60 µm thickness were imaged at the Vallisneri imaging facility (University of Padua, Padua, Italy) using the inverted optical microscope DM6 Leica (lesion volume quantification) or a Leica SP5 confocal laser scanning microscope (CLSM; Leica Microsystems, Inc., Wetzlar, Germany). For the microglia quantification, images were acquired with a 20x objective (NA: 0.50), 1.5 digital zoom. When applicable, the same parameters were used for the acquisition of the same image-category. For NeuN cell counting and microglia morphology, images were acquired with and objective of 63x in oil immersion (NA: 0.80). A Z-series of 13-30 optical sections spaced by 1 µm were acquired within each section. Individual images were averaged 2 times for each channel and merged by frames. The Hoechst staining was revealed with an excitation wavelength of 405 nm and emission wavelengths of 418–473 nm. The Alexa 488 staining was revealed with an excitation wavelength of 488 nm and emission wavelengths of 510–613 nm. The Alexa 568 staining was revealed with an excitation wavelength of 568 nm and emission wavelengths of 581-680 nm.

2.9 Analysis

2.9.1 Lesion volume quantification

One out of six images were analysed with ImageJ software by converting them in greyscale and adapting brightness and contrast. The lesion areas were traced in each section and the area measured. Finally, the lesion volume was computed with the following formula:

$$Lesion\ volume = \sum (Lesion\ area) * 0.06 * 6$$

where 0.06 was the width of each coronal section expressed in mm, and 6 was the distance factor (namely the distance between each brain slice).

The lesion index was computed with the following formula:

$$Lesion\ index = \sum (\frac{Lesion\ area}{Ipsilesional\ hemisphere\ area}) * 0.06 * 6 * 100$$

The shrinkage was computed with the following formula:

$$Shrinkage = \sum (\frac{Ispilesional\ hemishpere\ area}{Controlesional\ hemisphere\ area}) * 0.06 * 6 * 100$$

2.9.2 Cell density quantification: Iba-1 and NeuN

Images were acquired with a 20x objective by Leica SP5 confocal microscopy. The acquisitions were subsequently analysed on ImageJ software. In particular, images were processed to increase the contrast to allow the easily identification of microglia or post-mitotic neuronal cells, Iba-1 or NeuN positive cells, respectively. For neuronal quantification, confocal acquisitions were obtained in the ispilesional upper cortex, indicatively in layer 2/3 (L2/3) for both sham and stroke animals, and more specifically in the perilesional area for the latter ones. For microglia counting, confocal images were obtained from the both the brain hemisphere for both sham and stroke animals. Cell counting was performed manually from at least 4 brain slices from each animal per group, and the single values were averaged.

2.9.3 Microglia skeletonization: microglia morphology analysis

Microglia morphological analysis was performed by ImageJ software following the experimental procedure of Young and colleagues, 2018[30]. Briefly, z-stack of at least 30 μm^3 (with 2 µm steps) were acquired with 63x objective. 8-bit images were then processed on ImageJ to enhance contrast, remove noise and outliers and be converted into binary format. Finally, images were skeletonized by ImageJ plugin and the skeleton analysed (Fig. 12). The parameters assessed are branches average length per cell, mean soma's area and average endpoint voxels per cell.

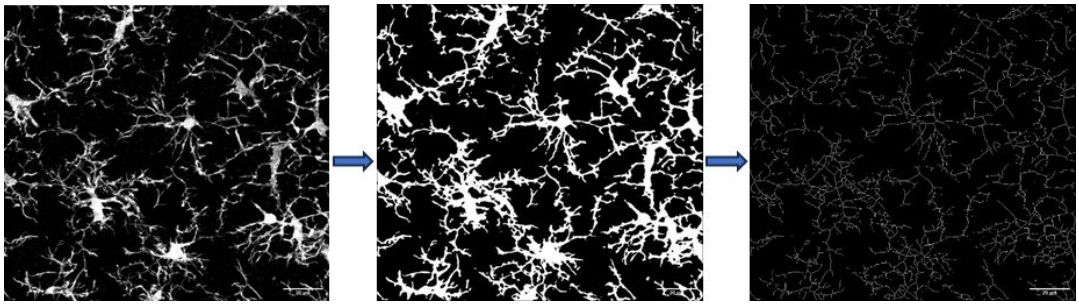

Figure 12. Qualitative representation of microglia skeletonization procedure. *Example confocal image processed (left), converted into a binary format (middle) and transformed for the skeleton analysis (right).*

2.9.4 Analysis of circulating cytokines

To investigate the systemic expression of the aforementioned analytes in the blood, the fold change logarithm (logFC) was computed as follows:

$$log2(FC) = log2(\frac{[analyte\ in\ stroke]}{[analyte\ in\ sham]}).$$

The cutoff for the determination of the statistically significant difference between the sham and stroke groups was performed computing the False Discovery Rate (FDR) as:

$$FDR(t) = E[V(t)]/E[S(t)]$$

and setting a confidence interval of 95%.

2.9.5 Stratification of stroked mice in good and poor recoverers

For each experimental day, the distribution of the sham group asymmetry index was used as baseline to stratify the stroke animals. Indeed, each stroke animal received a score from 0 to 2 according to the distance of its own asymmetry index value from the sham distribution mean. In particular, if the asymmetry index value was higher than 2 standard deviations (σ) from the sham mean, the animal received a score of 2. If the asymmetry index value was set in between 1.5 and 2σ from the sham mean, the animal received a score of 1.5. Animals with an asymmetry index value set in between 1 and 1.5σ from the sham mean received a score of 1. Finally, animals with an asymmetry index lower 1σ from the sham mean received a score of 0. Then, for each animal, I summed the scores of each experimental day, and obtained a global score of the asymmetric motor deficit. Ultimately, I set a threshold of 7.5 (based on the maximum score of the stroke animals) for the global motor score deficit to subdivide the stroked animals into two groups, good and poor recoverers.

2.11 Statistical analysis

Data are expressed as mean ± standard error of the mean (SEM). Shapiro-Wilk test and Levene test were performed on each dataset to confirm the normality of the dataset and homogeneity of variance. For two-groups comparisons, two-tailed Student's t or Wilcoxon-Mann-Whitney tests were used, depending on the data distribution. While when comparing more than 2 groups, One-way or Two-way analysis of variances (ANOVA) were used. Correlation analysis was performed computing the Pearson's correlation coefficient (significance level of $p < 0.05$). Cluster analysis was performed with the following parameters: column scaling, average linkage, Pearson distance.

3. Results

3.1 Validation of the dMCAO surgery: anatomical analysis

To induce an ischemic lesion at perinatal ages, mice underwent a stroke surgery at P14. Day P14 was chosen due to a higher probability to survive to the surgery. The distal medial cerebral artery occlusion (dMCAO; Fig. 13a) procedure causes the generation of a remarkable lesion principally located in the primary and secondary somatosensory cortices, representing the ischaemic core. However, the *penumbra* extends to the neighbouring motor cortices, likely affecting locomotor performances. To validate the dMCAO surgery procedure, I quantified the lesion volume of the animals perfused at P80 (stroke, n=8). Six out of eight animals displayed a significant lesion that I quantified as described in the methods section (Fig. 13b). Furthermore, the same group of animals was investigated for the shrinkage, defined as the reduction of the hemisphere volume after stroke. This strategy allowed me to quantify both the sham (n=10) and the stroke (n=8) groups, because no lesion was meant to be measured (Fig. 13c).

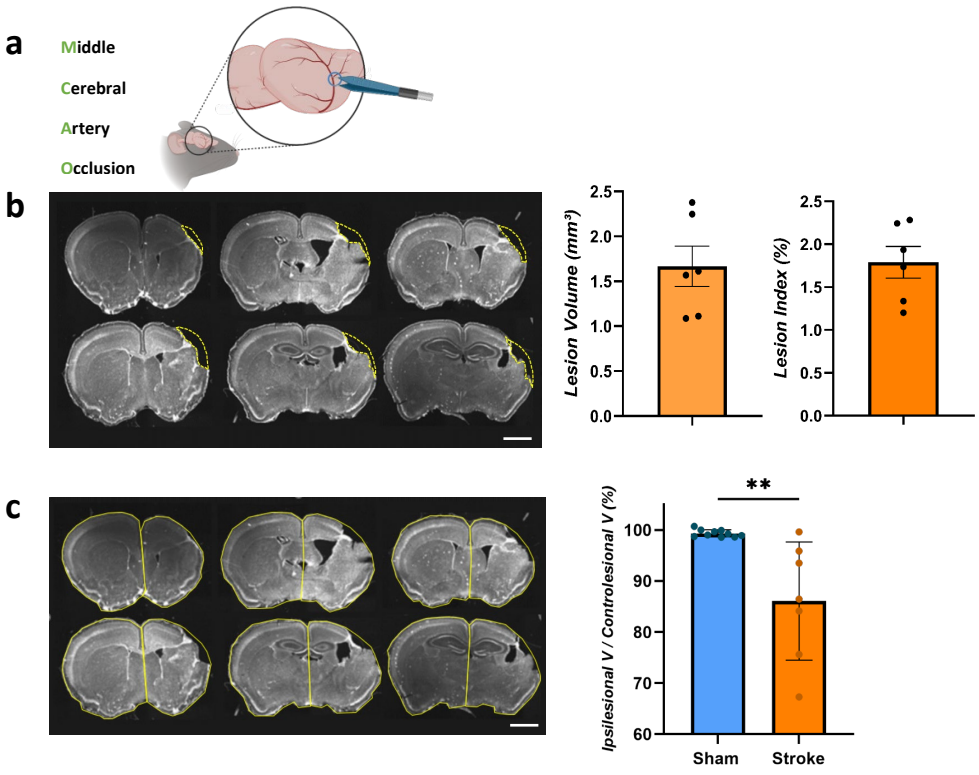

Figure 13. Histological assessment of dMCAO impacts on the brain. a) *Graphical representation of the distal middle cerebral artery occlusion technique.* ***b)*** *Left, representative mouse brain coronal slices stained with Hoechst Scale bar: 500µm. The*

yellow dashed area represents the lesion quantified with ImageJ. Middle, quantification of the lesion expressed in volume (n=6). Right, quantification of the lesion expressed as the percentage of the lesion area in the ipsilateral hemisphere (n=6) ***c)*** *Left, representative mouse brain coronal slices stained with Hoechst. Scale bar: 500µm. The yellow dashed lines represent the hemisphere contour used to compute the ipsilateral hemisphere shrinkage compared to the contralateral one. Right, quantification of the shrinkage in sham (blue, n=10) and stroke (orange, n=7) animals (Unpaired t-test, p < 0.01). ** P < 0.01.*

3.2 Perinatal stroke impacts on the fine motor behaviour later in life

With the aim to evaluate the impact of perinatal stroke on motor functions, I used the grid-walk test and assessed fine motor deficits at 2, 9, 23, 37, 51 and 79 days after stroke (Fig. 14a, 14b). Specifically, I computed the asymmetry index, defines as the difference between the percentage of left foot faults and the percentage of right foot faults, in sham and stroke groups. I found a higher asymmetry index in the stroke group compared to the sham at D23. Although the difference is not statistically significant at D2, D9, and 51 there is an evident trend of stroke mice to show higher motor impairments, potentially to be revealed by increasing the number of animals in each group.

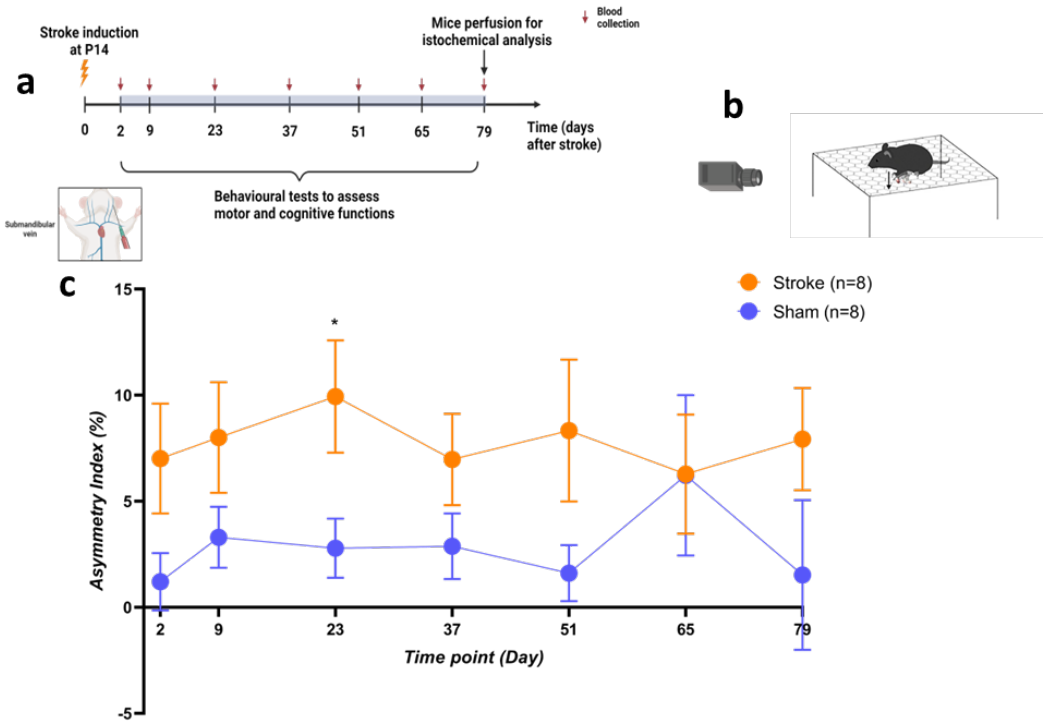

Figure 14. Perinatal stroke induces fine motor impairments. a) *Experimental timeline. dMCAO was induced at P14, followed by cognitive and motor behavioural testing at D2,*

D9, D23, D37, D51, D65 and D79 after stroke. In each time point, blood samples were collected for subsequent molecular analysis. At D79, mice were perfused for histochemical analysis. ***b)*** *Cartoon showing the grid-walk test.* ***c)*** *Quantification of the grid-walk test at different time points (2, 9, 23, 37, 51, 65 and 79 days after stroke) expressed as the percentage of asymmetry index for sham (blue, n=8) and stroke (orange, n=8) animals. Two-way ANOVA, HSD Tukey post hoc test, stroke vs sham D23, *P < 0.05.*

3.3 Brain damage and behavioural deficits correlation

To investigate possible correlations between behavioural deficits and the underlying anatomical lesion, I took advantage of a linear model and computed the Pearson correlation coefficient between the investigated variables. I found a positive correlation between the lesion index and the asymmetry index observed at D37 in stroke mice, suggesting that increasing the percentage of lesioned hemisphere, behavioural performances worse, as intuitively expected.

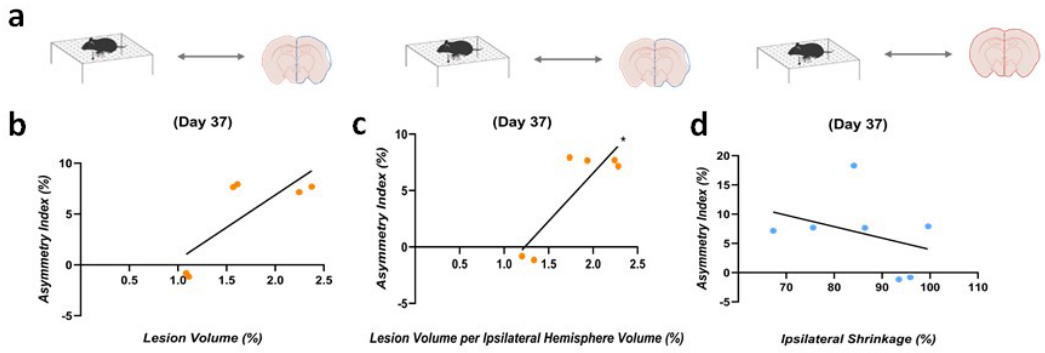

Figure 15. Correlation between motor impairments and anatomical lesion at D37. a) *Cartoon indicating the graphical correlation between the motor impairments (measured with the grid-walk test as asymmetry index) at D37 and the anatomical lesion (measured as lesion volume or lesion index or shrinkage).* ***b)*** *Correlation between the asymmetry index and lesion volume (Pearson's r= 0,7835).* ***c)*** *Correlation between asymmetry index and lesion index (Pearson's r= 0,8675).* ***d)*** *Correlation between asymmetry index and shrinkage (Pearson's r= -0,3458), *P < 0.05.*

3.4 PLX5622 treatment leads to microglia reduction in CD1 perinatal mouse

The second aim of the project was to investigate the role of the inflammatory response elicited by stroke through the microglia cells. To address this aim, a group of 10 mice were treated with PLX5622 for one week starting from day 1 after the stroke (n=7) or sham (n=3) surgery. The control groups received a vehicle solution

for the same time period after stroke (n=7) or sham (n=3) surgery. After one week of PLX or vehicle treatment, animals were perfused and the percentage of microglia reduction was evaluated. To check for the microglia depletion after PLX treatment, I used the Iba-1 biomarker, a cytoplasmatic protein frequently used for microglia detection. As shown with the staining for Iba-1, microglia were depleted by the PLX5622 treatment with a reduction of about 30% in both stroke and sham animals, compared to controls. Moreover, these results suggest that stroke itself does not alter microglia density.

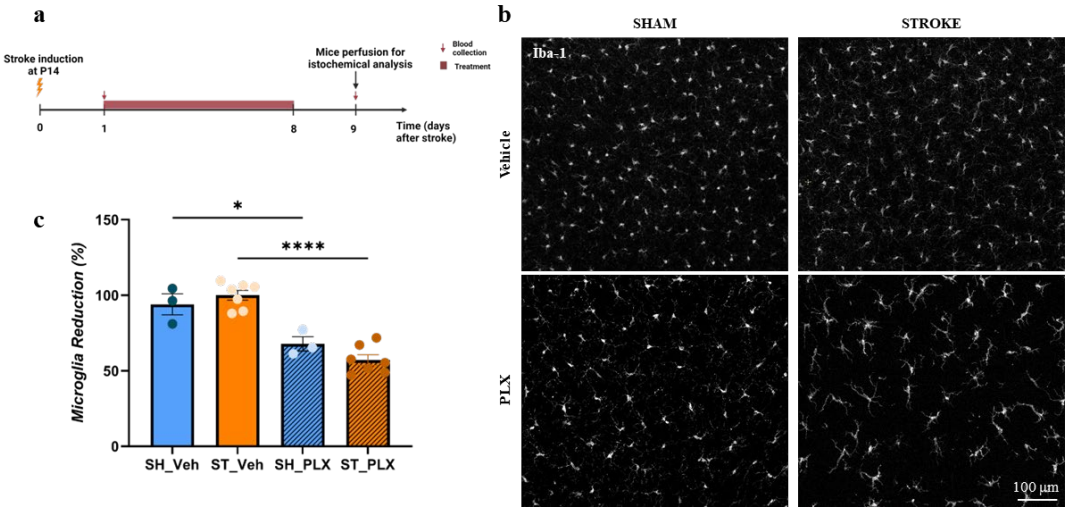

Figure 16. PLX5622 treatment led to microglia depletion. a) *Experimental timeline. Mice were treated with PLX-5622 from D1 to D8 after stroke induction and perfused at D9 for subsequent immunohistochemical analysis* ***b)*** *Representative confocal images showing microglia Iba-1 positive cells for sham (n=3) and stroke (n=7) vehicle groups or sham (n=3) and stroke (n=7) PLX-treated groups.* ***c)*** *Quantification of microglia depletion expressed as a reduction normalized to the stroke vehicle group. One-way ANOVA, HSD Tukey post hoc test, PLX vs vehicle sham, *P < 0.05; PLX vs vehicle stroke, ****P < 0.0001.*

3.5 Microglia-mediated inflammatory response quantification after stroke

I then assessed whether microglia depletion was associated with a reduction of the inflammatory response after the ischaemic insult. To achieve this aim, an immunohistochemical analysis (IHC) was performed targeting CD68. CD68 is a transmembrane glycoprotein of 110kD, which constitutes part of the

lysosomal/endosomal-associated membrane glycoprotein family (LAMP). It is involved in different functions, among which debris clearance, microglia recruitment and activation and phagocytosis[34], making it a commonly used biomarker for investigating neuroinflammation. Specifically, I performed a double staining with anti-Iba-1 and anti-CD68 (Fig. 17a), and I used two strategies. First, I quantified the ratio between the CD68 and Iba-1 mean fluorescence signals, and found no significant differences between the four conditions (Fig. 17b). Moreover, I analysed the CD68 mean fluorescence signal ratio between the ipsilesional and contralateral hemispheres (Fig. 17c). Although no statistically significant differences were observed, an overall trend of a higher inflammation in stroke vehicles as well as in sham and stroke PLX-treated animals can be detected. These preliminary results suggest that the PLX5622 treatment seems sufficient to promote neuroinflammation, even in absence of stroke induction. However, these results need to be further investigated (e.g. increasing the number of animals) and the potential increase of neuroinflammation further analysed (e.g. how many Iba-1 positive cells colocalize with CD68 and where[32]).

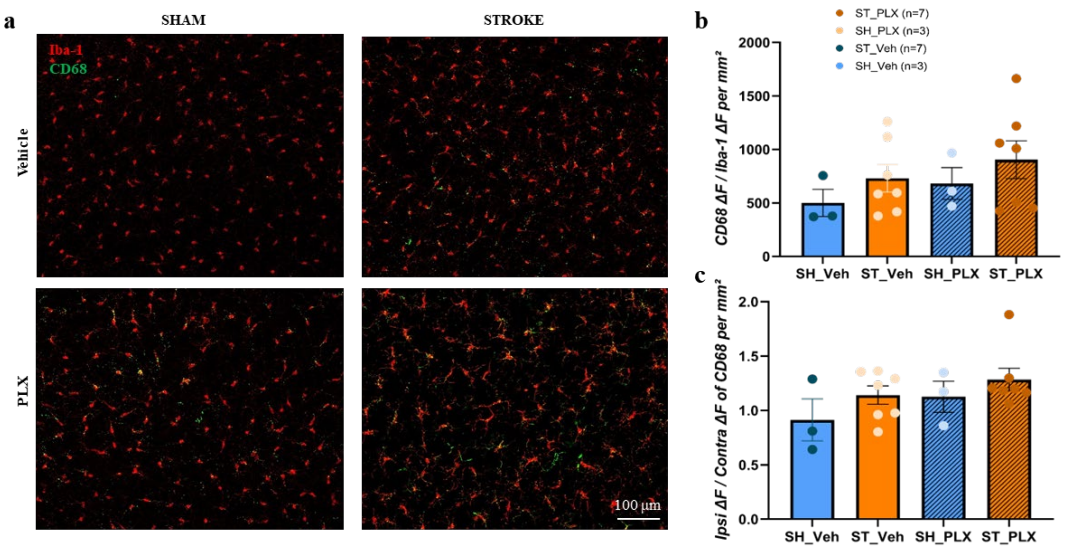

Figure 17. Neuroinflammatory response after ischaemic stroke. a) *Representative confocal images of double staining with anti-CD68 and anti-Iba-1 for sham (n=3) and stroke (n=7) vehicles, or sham (n=3) and stroke (n=7) PLX-treated groups.* ***b)*** *Quantification of the CD68 mean fluorescent signal normalized on Iba-1 mean fluorescent signal.* ***c)*** *Quantification of the CD68 mean fluorescent signal expressed as the ratio*

between ispilesional and controlesional hemispheres. One-way ANOVA, HSD Tukey post hoc test, not statistically significant.

3.6 Morphological characterization of microglia after stroke

When computing the density of Iba-1 positive cells, I noticed a specific morphology in the surviving microglia after PLX-treatment. As previously discussed, depending on the functional involvement, microglia can present several morphologies and phenotypes. To understand how microglia react to the different conditions (sham *versus* stroke, or vehicle *versus* PLX-treatment), I analysed its morphology in terms of branching degree, branch length and soma area (Fig. 18a-d) that I found statistically significant higher in the stroke PLX-treated animals compared to untreated ones. Surprisingly, I found a branch length increase and higher soma areas in sham PLX-treated animals, suggesting that the PLX-treatment alone was able to trigger a switch from a resting to an activated phenotype in microglia. This could be in accordance with previous observations indicating that PLX enhances microglia-mediated inflammatory response[27]. Another possibility can be that the reduction of the Iba-1 positive cells after PLX treatment can trigger the survival microglia to control a larger surrounding by extending their ramifications thus supporting the phenotype change.

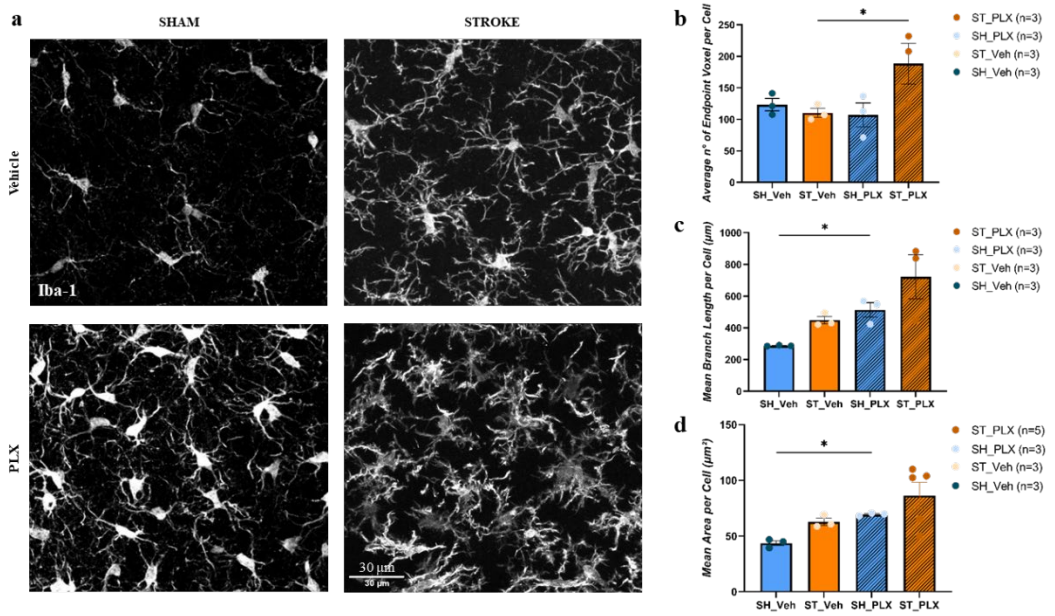

Figure 18. Morphological characterization of microglia. a) *Representative confocal images showing microglia Iba-1 positive cells.* ***b)*** *Quantification of the branching degree*

*(expressed as endpoint voxels). Kruskal-Wallis test, PLX vs vehicle stroke, *P < 0.05.* ***c)*** *Quantification of the branch length per cell. Kruskal-Wallis test, PLX vs vehicle sham, *P < 0.05.* ***d)*** *Quantification of the mean soma area per cell. Kruskal-Wallis test, PLX vs vehicle sham, *P < 0.05.*

3.7 Neuronal loss after stroke is worsened by the PLX5622 treatment

To assess the impact of the PLX-treatment on neurons following perinatal stroke, I performed the NeuN staining and computed the density of the neuronal population (Fig. 19a). As shown in Fig. 19, perinatal stroke led to neuronal loss in the perilesional region. Notably, the NeuN density reduction was also observed in PLX-treated animals, suggesting that PLX-treatment alone can induce a significant loss of neurons, independently of stroke. These results indicate that PLX5622 may exacerbate brain injury after stroke rather than ameliorate the pathological phenotype.

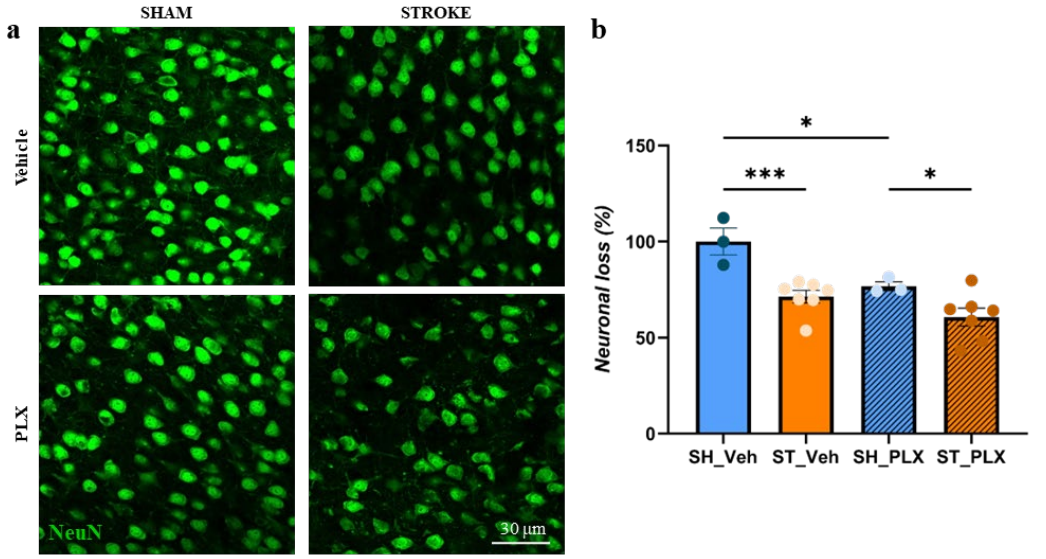

Figure 19. Neuronal loss after ischaemic stroke. a) *Representative confocal images showing the staining with anti-NeuN for sham (n=3) and stroke (n=7) vehicle groups, or sham (n=3) and stroke (n=7) PLX-treated groups.* ***b)*** *Quantification of the NeuN counting expressed as a reduction normalized to the sham vehicle group. One-way ANOVA, HSD Tukey post hoc test, sham vs stroke vehicle, ***P < 0.001; PLX vs vehicle sham, *P < 0.05; stroke vs sham PLX, *P<0.05.*

3.8 Systemic response to ischaemic perinatal stroke

To investigate the potential link between the central neuroinflammatory processes induced by the injury and the peripherical systemic consequences following an ischaemic perinatal event, I collected blood samples at 2, 9, 23, 37, 51 and 65 days (Fig. 14a) after stroke or sham surgery. Plasma samples of sham (n=8) and stroke (n=8) animals were then analyzed *via* the Luminex assay. Specifically, I first analysed the relative concentration of the 32 analytes by computing the logFC. Based on that, I found a statistically significant different expression of CCL11, IL-15 and CXCL5, which were respectively upregulated or downregulated according to the blue or red colour as represented in Fig. 20.

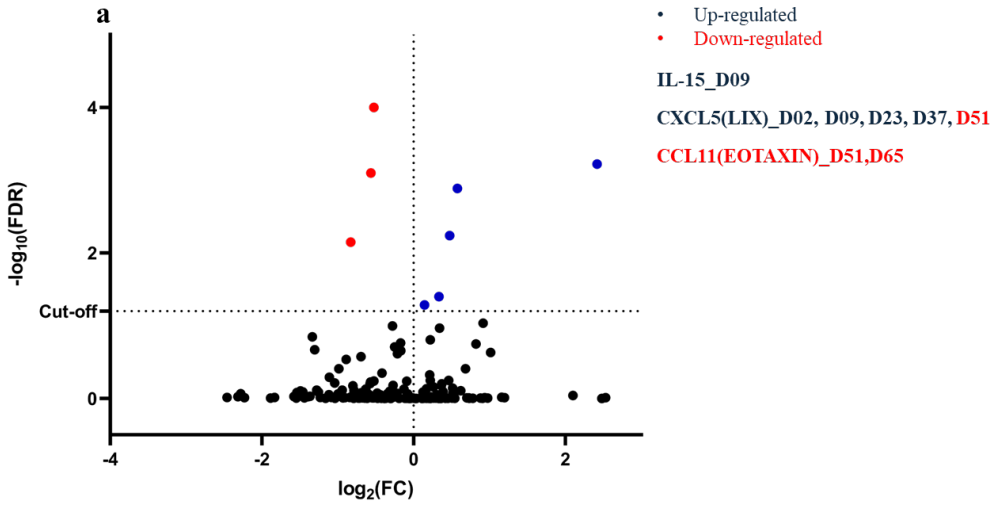

Figure 20. Relative expression of circulating cytokines in stroke and sham animals. *Quantification (volcano plot) of the relative expression between stroke and sham animals of the 32 blood analytes obtained via Luminex analysis at day 2, 9, 23, 37, 51 and 65 post-surgery. FDR = 0.05%.*

In particular, IL-15 was found to be upregulated in stroke animals compared to sham at day 9, corresponding to the stroke subacute phase (Fig. 21a). IL-15 absolves to many functions, among which the most important is the recruitment and proliferation of natural killer (NK) cells and lymphocytes T. This result indicates an increased activation of the adaptive component of the immune system in stroke animals compare to sham.

Pro-inflammatory cytokine C-C motif chemokine 11 (CCL11) expression was found to be lower in stroke compared to sham animals, during the chronic late phase (Fig. 21b). The CCL11 cytokine is a chemoattractant for CCR3 expressing cells, such as eosinophils, basophils, mast cells, Th2 lymphocytes and microglia. It is also involved in the regulation of the BBB permeability, modulating immune cells extravasation into the brain parenchyma. In humans, CCL11 is exploited as prognostic marker, indeed, it has been associated with neurogenesis and functional recovery[33].

Finally, CXC Motif Chemokine Ligand 5 (CXCL5) is pro-angiogenic factor. As reported by Fig. 21c, its expression in stroke animals is remarkably increased compared to sham ones from day 2 up to day 37, suggesting that one of the systemic processes activated by the central insult is the enhanced growth of new vessels in order to counteract the hypoperfusion following stroke.

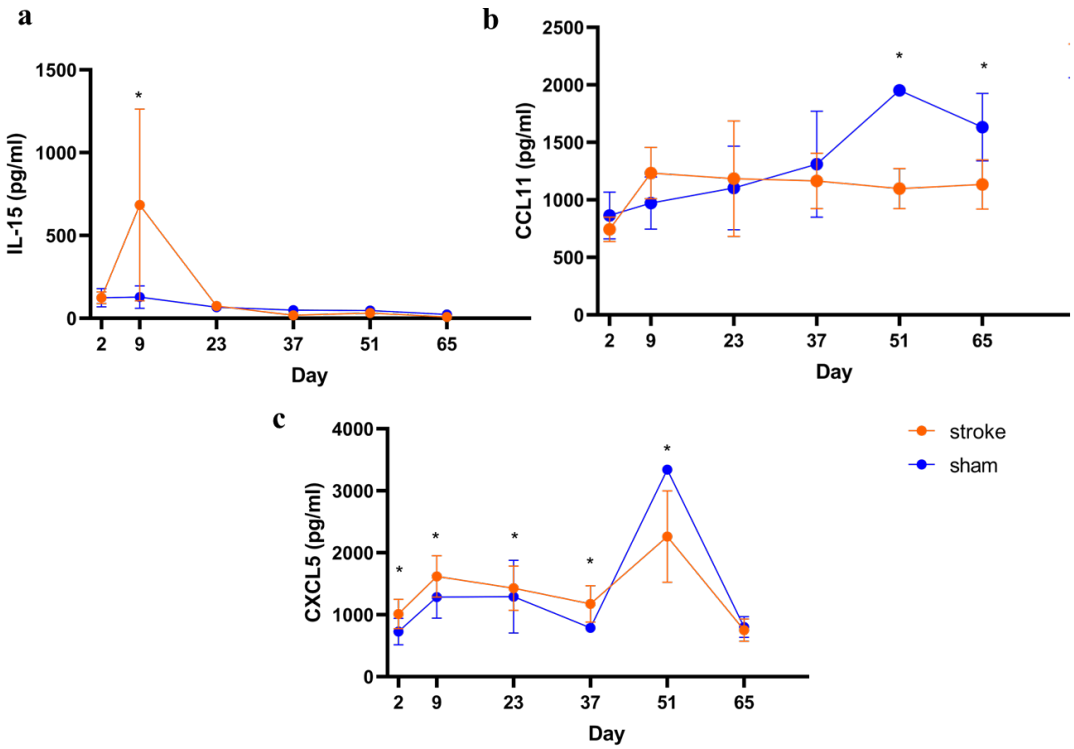

Figure 21. Relative expression of circulating cytokines in stroke and sham animals, across time. a) *IL-15 expression in stroke and sham animals at 2, 9, 23, 37, 51, and 65 days post-surgery. FDR = 0.05%.* ***b)*** *CCL11 expression in stroke and sham animals at 2, 9, 23, 37, 51, and 65 days post-surgery. FDR = 0.05%.* ***c)*** *CXCL5 expression in stroke and sham animals at 2, 9, 23, 37, 51, and 65 days post-surgery. FDR = 0.05%.*

3.9 Stratification of stroke animals in poor and good recoverers

With the aim to identify putative diagnostic or prognostic markers of ischaemic perinatal stroke, the stroke population was stratified as explained in the Materials and Methods section (paragraph 2.9.5). Based on the motor recovery outcome observed during the gridwalk test, I was able to identify three different sub-groups of stroked animals, poor (n=4) and good recoverers (n=4) (Fig. 22a, b).

a

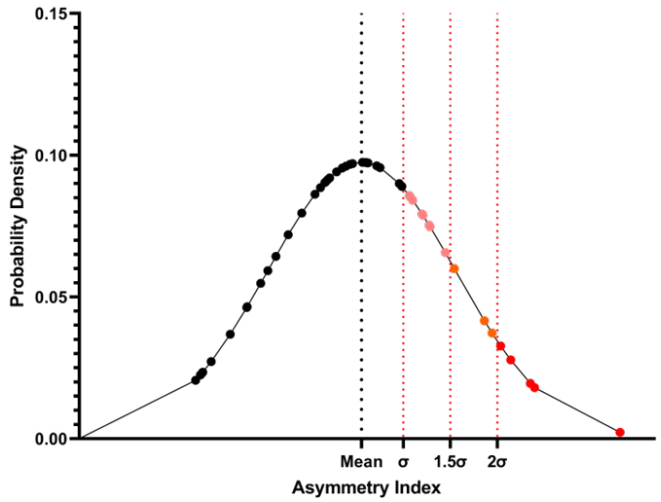

b

				σ	1.5σ	2σ		Poor	Good
	Day								
Sample		LV98	LV100	LV102	LV104	LV106	LV107	LV108	LV109
	2	12,39545998	4,545454545	18,25434971	1,708364451	7,96460177	7,510751075	1,989365603	-2,647837599
	9	9,239453357	11,49668365	7,19172757	10,23809524	5,390539054	14,5313681	-7,32946299	16,03688709
	23	10,9898909	14,33269863	9,716559891	9,450369155	18,23188947	10,47095386	-7,117647059	13,38834951
	37	-0,809716599	7,657657658	7,928802589	-1,158415842	7,692307692	18,30065359	7,159514925	8,96260338
	51	10,3912333	10,111023	9,239447578	8,680555556	4,242424242	22,73755656	-7,096774194	
	65	15,92108468	2,912621359	3,671790095	8,916666667	-5,882352941	8,21157218		7,760989011
	79	4,975728155	6,58008658	15,08218783	5,068728522	5,090909091	14,53208556	-6,666666667	1,917513844
	Motor Deficit Score	10,5	10	9	6	6,5	11,5	1,5	5,5

Figure 22. Stratification of stroke animals into good and poor recoverers. a) *Quantification of the asymmetry-index distance of the stroke animals from the mean distribution of the sham group. The curve (here exemplificative) represents the sham global asymmetry index distribution, and the circles represent the asymmetry-index values of each stroke animal. The circles are color-coded according to the distance of the asymmetry index value from the mean of the sham distribution in light (1σ), middle (1.5σ) and dark red (2σ). The dotted lines represent the asymmetry index mean value (black), and 1, 1.5 and 2σ standard deviation (red) from the mean of the sham group distribution.* ***b)*** *The table represents the final motor deficit score (MDS) assigned to each of the stroke animals based on their longitudinal performances during the overall experiment.*

3.9.1 Systemic response to ischaemic perinatal stroke in poor and good recoverers

To compare the cytokines profiles between the poor and good recovery outcomes groups, I used a cluster analysis and a heatmap to represent the results of the expression profiles (Fig. 23). I found that the stroke animals clustered into three groups at day 9 (Fig. 23), reflecting the recovery outcome stratification into poor and good. The mouse named as G3 (*LV108* in Fig. 22b) separately clustered in accordance with its global motor deficit score (MDS) (Fig. 22b). Indeed, in comparison with the other two groups which present very similar value of MDS, with a maximum variability of ±1.25 from the group mean value, G3 presents a very different value of MDS. To note that G3 motor performances were significantly distant from the sham mean only on day 37 (Fig. 22b), suggesting that this animal was particularly resilient to the brain injury (Fig. 13 and Fig. 22). Closer examinations are necessary to reveal the cellular and molecular peculiarities of this animal, characterizing the cause of its resilience. The same analysis performed on the cytokines profile of day 2 and 65 post surgery was not able to identify any significant cluster (data not shown).

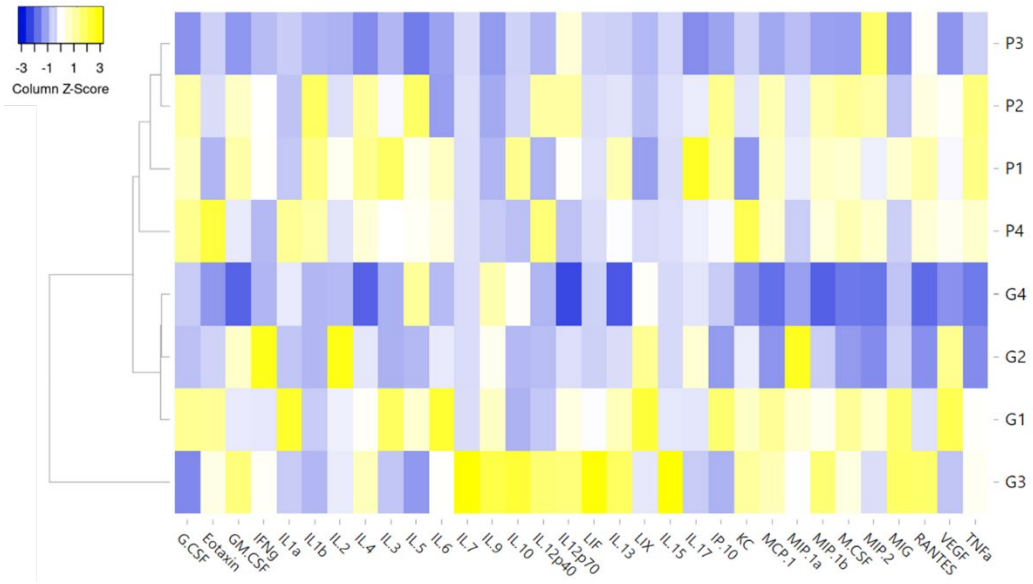

Figure 23. Cluster analysis of the cytokines profile expression for poor and good recoverers. *The heatmap shows the results of the cluster analysis performed on the cytokines profile expressions at day 9 of poor and good recovery outcome groups. P1, P2, P3 and P4 belong to the Poor recovery outcome group, while G1, G2, G3 and G4 belong*

to the Good recovery outcome group. The colour scale indicates the increase (yellow) or decrease (blue) of the cytokine expression levels.

Subsequentially, I analysed the factors which better describe the discrimination between the two groups. As shown in Fig. 24, the statistically significant difference between good and poor recoverers at day 9 is mainly driven by IL-15 and CXCL5(LIX) expression levels. Specifically, both factors are overexpressed in good recoverers compared to the poor ones. Globally, these results suggest that, after stroke, the motor recovery outcome of each mouse across time is positively correlated with the concentration of pro-angiogenic factors (CXCL5) and immune cells recruiting factors (IL-15) during the first week (late-acute phase) post stroke. Despite that, further research are needed to obtain a more comprehensive view of the systemic response to perinatal stroke.

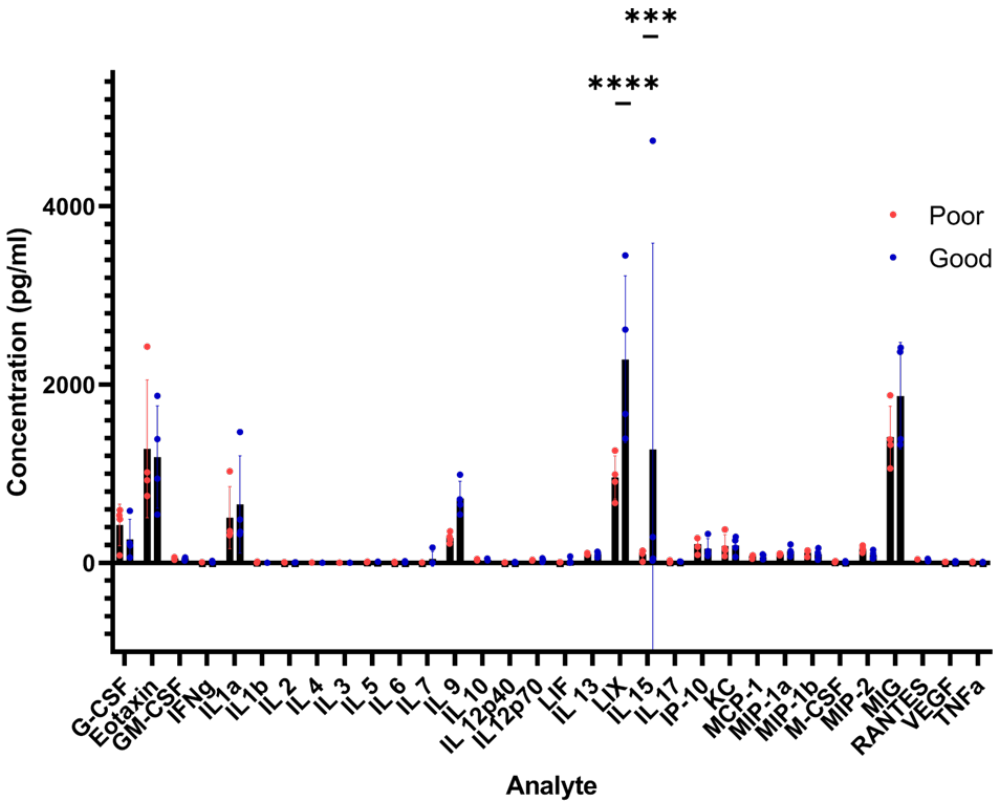

Figure 24. Cytokines profile expression in poor and good recoverers at D9. *The scatterplot represents the comparison of cytokines mean concentration at day 9 between poor and good stroke recoverers. One-way ANOVA, HSD Tukey post hoc test, CXCL5(LIX) poor vs good, ****P < 0.0001; IL-15 poor vs good, ***P < 0.001.*

3.10 Correlation between cytokines expression levels and ischemic lesion

To investigate whether the cytokines expression levels could explain the anatomical damage, I correlated each analyte expression with the lesion size of each animal. I observed that the correlation between the anatomical damages and the circulating cytokines concentration has revealed a significant correlation with granulocytes colony stimulator factor (G-CSF). G-CSF is an important growth and survival factor of immune cells belonging to the granulocyte's family.

More specifically, I observed a linear positive correlation between G-CSF measured at day 2 and the lesion volume at day 79, and a linear negative correlation between shrinkage and G-CSF at day 2 (Figure 25a, 25b). According to the hypothesis that the concentration of G-CSF could be associated with the intensity of the immune response, this result suggests that G-CSF concentration could be exploited as a prognostic marker. Furthermore, this result confirms the initial hypothesis that downregulating the acute immune response would ameliorate post stroke outcomes.

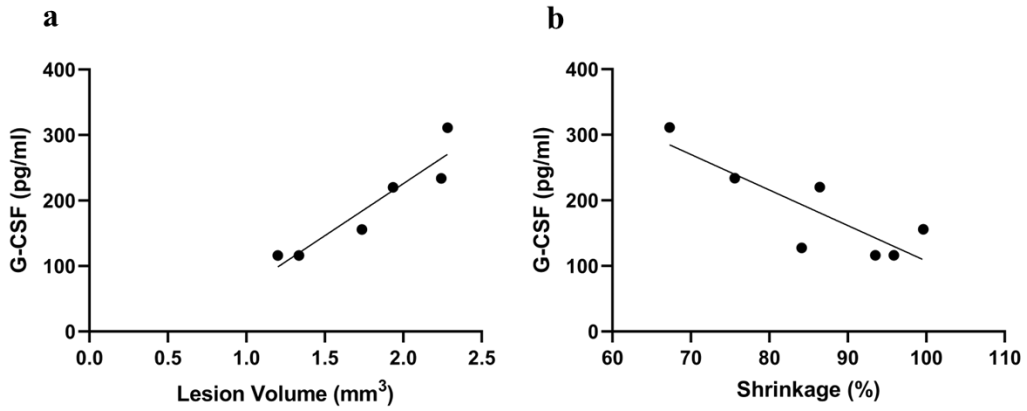

***Figure 25. Correlation between anatomical damages and cytokines blood concentration at day 2 post-surgery**. **a)** Correlation between G-CSF blood concentration at day 2 and lesion volume (Pearson's r = 0,9353). **b)** Correlation between G-CSF blood concentration at day 2 and shrinkage (Pearson's r = -0,8417).*

4. Discussion

In my thesis project I investigated the microglia-mediated neuroinflammation in a mouse model for perinatal stroke. Several considerations must be made regarding this study.

4.1 The dMCAO animal model

First of all, the dMACO technique was shown to be suitable to induce an ischaemic stroke in a mouse model. dMCA occlusion is sufficient to generate a significant cortical lesion which is often accompanied by the shrinkage of the ipsilesioned hemisphere. As reported from other studies of adult stroke, the lesion mainly localizes in the primary and secondary somatosensory cortices, while the penumbra extends to the motor cortices.

As previously discussed, ischaemic stroke represents the prevalent form of stroke in humans, and more than one-half of them occur in the MCA territory[2], making the mouse model described in this project suitable for preclinical studies. However, it has been shown that cortical lesions account for approximately 15% of the total number of stroke-induce damages in humans[2]. Based on that, the dMCAO technique may be not suitable to model the subcortical injuries induce by stroke. Although the cortical localization, I sometimes observed the presence of a glial scar in the white matter (highlighted by the GFAP staining), suggesting that the insurgency of subcortical lesion following dMCAO could occur. This aspect needs to be further investigated, for example with a staining for MBP (myelin-basic protein) to quantify the potential myelin density reduction following stroke.

4.2 Assessment of the behavioural functional recovery after perinatal stroke

Another important consideration is related to the mouse behavioural testing. The behaviour may be heavily subjected to strain-dependent fluctuations, leading to different outcomes. Accordingly, to establish a complete validation of the motor consequences of the perinatal stroke model, it would be fundamental to characterize the behavioural profile of the underlying mouse strain[31].

Different motor tests for the detection of unilateral motor impairments have been developed to characterized mice motor phenotype in different pathological

conditions. Grid-walk test is a well diffuse suitable sensorimotor test to reveal fine unilateral motor deficits induces by focal cortical lesions[31]. Regardless of that, grid-walk test presents some disadvantages, as fine motor impairments could be hidden if animals adopt compensatory movement strategies to perform the task. Moreover, since that the majority of the lesion affect the somatosensory cortices, it would be interesting to apply different behavioural tests capable to assesses eventual defects of the somatosensory system induce by the ischaemic insult. For example, Ishmail Abdus-Saboor and colleagues (2022)[31], assessed mice somatosensory behaviour *via* high-speed videography behavioural setup, giving as input different sensory stimuli and characterizing mice sensory experience.

4.3 The role of microglia during neurodevelopment in health and disease

Eventually, a fundamental consideration must be done on PLX-5622 treatment. As previously discussed, microglia are fundamental to maintain brain function, working as homeostatic housekeeper. Their importance is well known in both brain physiology, where they accomplish to several processes critically interacting with other cell types, and pathology, where they act as adaptive responders to brain injuries to restore the physiological conditions[32]. Furthermore, microglia play a critical role during brain development and wiring[32]. They are actively involved in neuronal apoptosis, neurogenesis, synaptic pruning, synaptogenesis, and synaptic transmission; indeed, they are currently considered as the fourth component of the so called "quad-partite synapse" [32]. Growing evidence suggest that microglia perturbation during brain maturation are sufficient to drastically delay brain wiring and neuronal development, promoting several dysfunctions. Based on the developmental stage and the duration of microglia depletion, different effects have been observed on synapse functions *in vivo*, as well as on neuronal circuits[32]. Early-post-natal microglia ablation can also lead to long-lasting deficits in anxiety, social and locomotor behaviour[32]. Significant neuronal death in cortical layer V has been observed in Cd11b-DTR mouse line after transient microglia depletion at postnatal day 3 [32]. Another study reported a significant reduction of synaptic pruning and genesis after microglia depletion, associated with perturbations of synaptic protein levels. Microglia ablation in adulthood induces a milder phenotype, suggesting that

microglia-mediated synaptic remodelling is mainly confined to the first post-natal weeks[32].

4.3.1 Impact of the microglia depletion after perinatal stroke

Several studies suggest a beneficial role of microglia transient depletion in pathological conditions. For example, it has been observed that long-term microglia depletion using CSF1R inhibitor PLX-5622 induces a rise of the overall spine density, enhancing excitatory post-synaptic current amplitude[32]. A further important result derived from the work of C. Bourget and colleagues (2022)[29], who demonstrated that microglia ablation with PLX-5622 efficiently led to a significant improvement of mice locomotor outcomes after neonatal ischaemic stroke[29].

Several microglia depletion models, both *via* pharmacological and genetic methods, have been developed. Among the pharmacological methods to ablate microglia, the most commonly used are the administration of toxic clodronate-containing liposomes[35], or the inhibition of factors necessary for microglia survival and maturation, such as the CSF1 or PU.1[32]. Other approaches exploit the expression of suicidal genes, such as the diphtheria toxin receptor (DTR) or viral thymidine kinase (HSVTK), which expression is controlled by microglia specific promoters, as CD11b or Cx3CR1. The advantage of pharmacological methods is to have a fine control on treatment timing and dose. Moreover, pharmacological ablation is transient, and microglia is capable of rapidly repopulating the brain parenchyma after drug elimination[32]. Genetic models of microglia depletion are mainly represented by constitutive knockout of critical transcriptional or survival factors (PU.1 KO, CSF1R KO, TGFβ KO), offering approaches to obtained long-lasting microglia ablation. However, several important complications emerged from microglia fundamental role during neurodevelopment. This problem was overcame exploiting inducible genetic microglial-specific CRE lines to induce microglia depletion later on during the development. Despite that, an important complication regarding these kinds of approaches is represented by the absence of fully microglia-specific promoters employed, leading to off-side effects[32].

As previously discussed, I treated mice with PLX-5622 for a week after stroke induction with the aim to reduce the neuroinflammatory response and ameliorate

the functional recovery. Unfortunately, different complications emerged during the experiment. First of all, I found several difficulties during the preparation of the PLX-5622 solution, because of its low solubility in a hydrophilic medium. Based on that, the drug preparation protocol is very sensible to any environmental perturbations, such as the temperature, and does not allow to store the solubilized drug. Moreover, the hydrophobic nature of the PLX-5622 forced me to use elevated concentration of high-density compounds to solubilize the drug. This created an additional complication, for example the daily administration of PLX-5622 by intraperitoneal injections was difficult to control because of the high-density of the final solution to inject.

Microglia repopulation after transient ablation with PLX-3397 occur very rapidly in adult mice[32]. Indeed, it has been observed an important repopulation within three days after inhibitor withdrawal, with an important proliferation already occurring after two days. Moreover, one day after treatment cessation, drug was almost completely cleared from the brain, with only traces still detectable. Furthermore, the surviving microglia presented a larger soma and increased thickness of branches, typically associated with a reactive phagocytic phenotype[32]. Considering that the drug I used is slightly different and that I worked on a neonatal model, the balance between drug-mediated ablation and microglia repopulation could be different. This opens to the possibility that microglia were not efficiently depleted, inducing the remaining microglia cells to acquire a reactive pro-inflammatory phenotype and exacerbating the brain injury. This idea is supported by the significantly lessened reduction we obtained compared to literature, on average 60% against almost 90% depletion as reported by other studies. In addition, microglia proliferative capabilities may be enhanced during developmental stage, thanks to the presence of highly proliferative progenitors[32].

Importantly, the observed neuronal death after PLX treatment must be investigated. Indeed, the drug may present a cell-type specific effect, targeting preferentially specific neurons and possibly unbalancing the excitatory/inhibitory activity ratio. Such process would worse the animal conditions, increasing the susceptibility to co-morbidities, such as epilepsy. On the other hand, neuronal loss may play a beneficial role. In fact, a brain damage may induce to several aberrant mechanisms

of neuroplasticity, promoting negative forms of neuronal circuitry reorganization that can ultimately affects brain functions. In this scenario, whether PLX has a beneficial or detrimental role remains to be explored.

Finally, targeting the CSF1R pathway may have significant side effects on other cells of the myeloid lineage. For example, hematopoietic stem cells, macrophages, osteoclasts and mast cells express this important survival receptor[32]. It would be interesting to investigate the PLX-5622 impact on other cell types. Further analyses are necessary to reveal if the worsened observed phenotype of the treated mice is due to a causative relationship with PLX-5622 treatment.

4.4 Systemic response following perinatal ischaemic stroke

Blood analytes analysis represents a remarkable tool for the investigation of the systemic immune response following an injury and during the pathophysiological development of a disease. In particular, the circulating factor's contribution in the pathophysiological processes following ischaemic stroke is usually exploited for diagnostic and prognostic porpoises in humans. Indeed, from this relatively cheap and rapid analysis, it is possible to obtain a huge amount of information which allows to better understand the specific pathological processes occurring in each patient and develop a subject specific treatment.

For example, CCL11 blood concentration is exploited as predictor of neurogenesis and long-term functional outcomes in patients following ischaemic stroke. More specifically, it has been observed that lower CCL11 blood levels during the chronic phase are predictive of increased stroke severity and poorer functional outcomes in stroke patients[34]. Notably, intraperitoneal injections of CCL11 promote neurogenesis in adolescent mice while it exacerbates brain injury in adult mice[33]. The contraposition of these results highlights the complexity of the interpretation of this analysis. Indeed, specific analytes can fulfil different processes even with opposite outcomes based on the species, the developmental stage, the interaction with other factors or the disease.

CXCL5 is a chemokine which belongs to the CXC subtype, binding with CXCR2 to promote angiogenesis and remodelling connective tissue by recruiting neutrophils. It has been reported that CXCL5 is upregulated following ischaemic

stroke in humans, despite the exact meaning remain unclear. It has been reported that *in vitro* anti-CXCL5 treatment targeting human brain microvascular endothelial cells (BMECs) promotes cell proliferation and reduces cell permeability, suggesting that CXCL5 silencing attenuated ischaemic/hypoxic-induced injury in human BMECs[35]. These results are in contrast with the observation of a positive correlation between circulating CXCL5 levels and motor recovery which I observed in perinatal mice.

G-CSF is well known to be a fundamental modulator of the granulopoiesis, remarkably influencing both myeloid and non-myeloid immune cells. G-CSF upregulation has been observed in different cancer types such as breast cancer, bladder cancer, glioma and neuroblastoma, acting primarily through the JAK/STAT pathway and modulating tumour proliferation, migration and metastasis.

In particular, it works as a survival factor for microglia cells, competing for the binding to the CSFRs with the PLX5622. The positive correlation between lesion volume and G-CSF blood levels during the acute phase suggests that the modulation of the early immune response following stroke would be a great target to improve stroke outcomes. Further analyses are necessary to reveal the link between the G-CSF levels and the anatomical damages.

In conclusion, it is important to underlight that the knowledge transponibility from one species to another is not always possible, therefore it is fundamental to identify the differences and similarities in order to exploit the awareness acquire in mice and to translate them in humans.

5. Conclusion and Future Perspectives.

In conclusion, this study demonstrated the suitability of the dMCAO technique to explore at different levels the pathological outcomes of ischaemic stroke in a mouse model at perinatal ages.

PLX-5622 treatment efficiently depleted microglia cells but it parallelly promoted a series of effects. Among them, it primed microglia to acquire a hyper-ramified phenotype and promoted neurons degeneration. Microglia phenotype switch has to be better looked into, given that microglia hyper-ramification is related both to restoration and inflammation based on the specific context[27]. The consequences of the treatment on the mice behavioural performances are still unknown, although the anatomical impact of PLX-5622 likely suggests a worsening of mice functional recovery after stroke. Despite that, further analyses will be necessary to confirm these results, getting insight into the molecular mechanisms underlying the observed phenotype.

During my internship, I performed the grid-walk test in a subset of stroke animals treated with PLX-5266 (n=3) or vehicle (n=2) to assess whether the PLX-treatment could ameliorate the behavioural recovery outcome following perinatal stroke (Fig. 26a). Preliminary results are shown in Fig. 26b, more animals need to be processed and the data analysis are still ongoing.

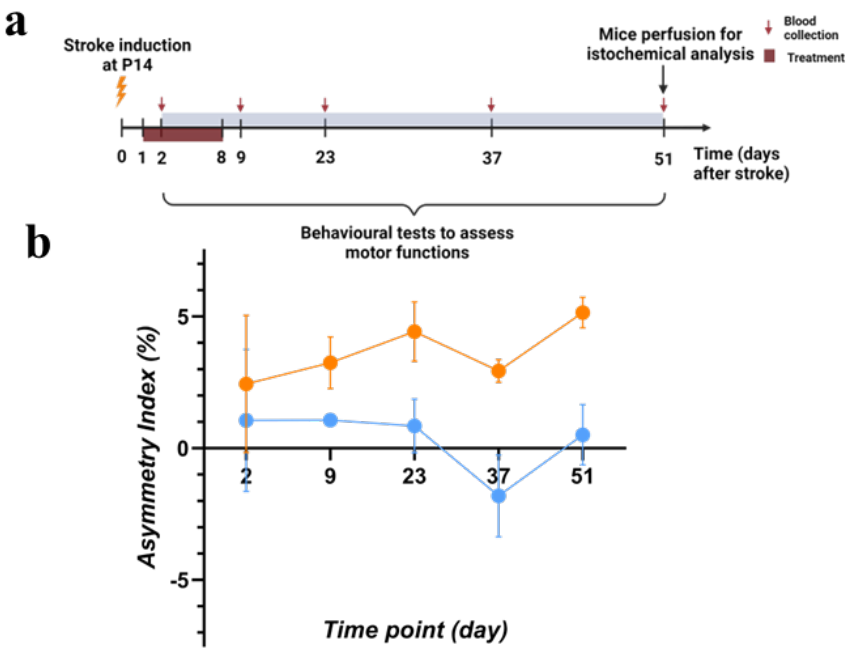

Figure 26. Assessment of motor and cognitive functions after PLX-5622 treatment. a) *Experimental timeline. Mice were treated with PLX-5622 or vehicle from D1 to D8 after stroke induction. Subsequently, mice were behaviourally tested at D2, D9, D23, D37 and D51 after stroke induction.* ***b)*** *Quantification of the grid-walk test expressed as the percentage of asymmetry index at D2, D9, D23, D37 and D51 after stroke, for untreated (blue, n=2) and treated (orange, n=3) stroke groups. Two-way ANOVA wad applied to determine the differences between group means.*

Another aspect that I started to work during my internship was to investigate the inflammatory systemic responses induced by the ischemic lesion and the possible correlation with the CNS injury. To achieve this aim, blood samples were collected during each behavioural time point. This result will give us important information about the inflammatory signalling potentially activated at the systemic level and mirrored by the local microglia-mediated neuroinflammation. Overall, this project will reveal the putative association between CNS neuroinflammation, systemic response and functional recovery after perinatal stroke, thus opening new intervention strategies to the pre-clinical therapeutic development.

6. References

1. Bingbing Lin, Mengxue Wang, Xiaocheng Chen, Linsong Chai, Jinglei Ni, Jia Huang, Involvement of P2X7R-mediated microglia polarization and neuroinflammation in the response to electroacupuncture on post-stroke memory impairment, Brain Research Bulletin, Volume 212, 2024, 110967, ISSN 0361-9230, https://doi.org/10.1016/j.brainresbull.2024.110967.

2. Campbell, B.C.V., De Silva, D.A., Macleod, M.R. *et al.* Ischaemic stroke. *Nat Rev Dis Primers* **5**, 70 (2019). https://doi.org/10.1038/s41572-019-0118-8.

3. Feigin, V. L. et al. Global, regional, and country-specific lifetime risks of stroke, 1990 and 2016. N. Engl. J. Med., (2018).

4. Feigin VL, Krishnamurthi RV, Parmar P, Norrving B, Mensah GA, Bennett DA, Barker-Collo S, Moran AE, Sacco RL, Truelsen T, Davis S, Pandian JD, Naghavi M, Forouzanfar MH, Nguyen G, Johnson CO, Vos T, Meretoja A, Murray CJ, Roth GA; GBD 2013 Writing Group; GBD 2013 Stroke Panel Experts Group. Update on the Global Burden of Ischemic and Hemorrhagic Stroke in 1990-2013: The GBD 2013 Study. Neuroepidemiology. 2015;45(3):161-76. doi: 10.1159/000441085. Epub 2015 Oct 28. PMID: 26505981; PMCID: PMC4633282.

5. Rocha, M. & Jovin, T. G. Fast versus slow progressors of infarct growth in large vessel occlusion stroke: clinical and research implications. *Stroke* **48**, 2621–2627 (2017).

6. Bernhardt, J., Hayward, K.S., Kwakkel, G., Ward, N.S., Wolf, S.L., Borschmann, K., et al. (2017) Agreed definitions and a shared vision for new standards in stroke recovery research: the Stroke Recovery and Rehabilitation Roundtable taskforce. International Journal of Stroke, 12(5), pp. 444–450. https://doi.org/10.1177/1747493017711816.

7. DiSabato DJ, Quan N, Godbout JP. Neuroinflammation: the devil is in the details. J Neurochem. 2016 Oct;139 Suppl 2(Suppl 2):136-153. doi: 10.1111/jnc.13607. Epub 2016 May 4. PMID: 26990767; PMCID: PMC5025335.

8. Nowak, L., Bregestovski, P., Ascher, P., Herbet, A. & Prochiantz, A. Magnesium gates glutamate-activated channels in mouse central neurones. *Nature* **307**, 462–465 (1984).

9. Rabiller G, He JW, Nishijima Y, Wong A, Liu J. Perturbation of Brain Oscillations after Ischemic Stroke: A Potential Biomarker for Post-Stroke Function and Therapy. Int J Mol Sci. 2015 Oct 26;16(10):25605-40. doi: 10.3390/ijms161025605. PMID: 26516838; PMCID: PMC4632818.

10. Xu S, Lu J, Shao A, Zhang JH, Zhang J. Glial Cells: Role of the Immune Response in Ischemic Stroke. Front Immunol. 2020 Feb 26;11:294. doi: 10.3389/fimmu.2020.00294. PMID: 32174916; PMCID: PMC7055422.

11. Joseph L. Cheatwood, April J. Emerick, Martin E. Schwab and Gwendolyn L. Kartje, Nogo-A Expression After Focal Ischemic Stroke in the Adult Rat, Originally published8 May 2008, https://doi.org/10.1161/STROKEAHA.107.507426Stroke. 2008;39:2091–2098

12. Hall, C. N. et al. Capillary pericytes regulate cerebral blood flow in health and disease. Nature 508, 55–60 (2014).

13. Chamorro, Á., Meisel, A., Planas, A. *et al.* The immunology of acute stroke. *Nat Rev Neurol* **8**, 401–410 (2012). https://doi.org/10.1038/nrneurol.2012.98.

14. Maysami, S. et al. A cross-laboratory preclinical study on the effectiveness of interleukin-1 receptor antagonist in stroke. J. Cereb. Blood Flow Metab. 36, 596–605 (2016).

15. Ko, N. U. in *Aminoff's Neurology and General Medicine* (ed. Aminoff, M. J.) 183–198 (Academic Press, 2014).

16. Desowska, A. & Turner, D. L. Dynamics of brain connectivity after stroke. Rev. Neurosci. 30, 605–623 (2019).

17. Jin, K. et al. Evidence for stroke-induced neurogenesis in the human brain. Proc. Natl Acad. Sci. USA 103, 13198–13202 (2006).

18. Emberson, J. et al. Effect of treatment delay, age, and stroke severity on the effects of intravenous thrombolysis with alteplase for acute ischaemic stroke: a

meta-analysis of individual patient data from randomised trials. Lancet 384, 1929–1935 (2014). A meta-analysis of individual patient data from intravenous thrombolysis trials that emphasizes the important influence of time to treatment on patient outcomes.

19. Powers, W. J. et al. 2018 guidelines for the early management of patients with acute ischemic stroke: a guideline for healthcare professionals from the American Heart Association/American Stroke Association. Stroke 49, e46–e110 (2018).

20. Campbell, B. C. V. et al. Effect of general anaesthesia on functional outcome in patients with anterior circulation ischaemic stroke having endovascular thrombectomy versus standard care: a meta-analysis of individual patient data. Lancet Neurol. 17, 47–53 (2018).

21. Whitaker EE, Cipolla MJ. Perinatal stroke. Handb Clin Neurol. 2020;171:313-326. doi: 10.1016/B978-0-444-64239-4.00016-3. PMID: 32736758.

22. Heléne E.K. Sundelin, Anna Walås, Jonas Söderling, Peter Bang and Jonas F. Ludvigsson, Long-Term Mortality in Children With Ischemic Stroke: A Nationwide Register-Based Cohort Study, Originally published 8 Dec 2021. https://doi.org/10.1161/STROKEAHA.121.034797Stroke. 2022;53:837–844.

23. Gao, C., Jiang, J., Tan, Y. *et al.* Microglia in neurodegenerative diseases: mechanism and potential therapeutic targets. *Sig Transduct Target Ther* **8**, 359 (2023). https://doi.org/10.1038/s41392-023-01588-0.

24. Vitry S, Bertrand JY, Cumano A, Dubois-Dalcq M. Primordial hematopoietic stem cells generate microglia but not myelin-forming cells in a neural environment. J Neurosci. 2003 Nov 19;23(33):10724-31. doi: 10.1523/JNEUROSCI.23-33-10724.2003. PMID: 14627658; PMCID: PMC6740906.

25. Ginhoux, F. et al. Fate mapping analysis reveals that adult microglia derive from primitive macrophages. *Science* **330**, 841–845 (2010).

26. Tabitha R F Green, Rachel K Rowe, Quantifying microglial morphology: an insight into function, Clinical and Experimental Immunology, Volume 216, Issue 3, June 2024, Pages 221–229, https://doi.org/10.1093/cei/uxae023

27. Smith KL, Kassem MS, Clarke DJ, Kuligowski MP, Bedoya-Pérez MA, Todd SM, et al. . Microglial cell hyper-ramification and neuronal dendritic spine loss in the hippocampus and medial prefrontal cortex in a mouse model of PTSD. Brain Behav Immun 2019, 80, 889–99. doi:10.1016/j.bbi.2019.05.042.

28. Shui X, Chen J, Fu Z, Zhu H, Tao H, Li Z. Microglia in Ischemic Stroke: Pathogenesis Insights and Therapeutic Challenges. J Inflamm Res. 2024 May 22;17:3335-3352. doi: 10.2147/JIR.S461795. PMID: 38800598; PMCID: PMC11128258.

29. Bourget, C., Adams, K.V. & Morshead, C.M. Reduced microglia activation following metformin administration or microglia ablation is sufficient to prevent functional deficits in a mouse model of neonatal stroke. J Neuroinflammation 19, 146 (2022). https://doi.org/10.1186/s12974-022-02487-x.

30. Young, K., Morrison, H. Quantifying Microglia Morphology from Photomicrographs of Immunohistochemistry Prepared Tissue Using ImageJ. J. Vis. Exp. (136), e57648, doi:10.3791/57648 (2018).

31. Conti E, Piccardi B, Sodero A, Tudisco L, Lombardo I, Fainardi E, Nencini P, Sarti C, Allegra Mascaro AL, Baldereschi M. Translational Stroke Research Review: Using the Mouse to Model Human Futile Recanalization and Reperfusion Injury in Ischemic Brain Tissue. Cells. 2021 Nov 25;10(12):3308. doi: 10.3390/cells10123308. PMID: 34943816; PMCID: PMC8699609.

32. Paolicelli RC, Ferretti MT. Function and Dysfunction of Microglia during Brain Development: Consequences for Synapses and Neural Circuits. Front Synaptic Neurosci. 2017 May 10;9:9. doi: 10.3389/fnsyn.2017.00009. PMID: 28539882; PMCID: PMC5423952.

33. Lieschke S, Zechmeister B, Haupt M, Zheng X, Jin F, Hein K, Weber MS, Hermann DM, Bähr M, Kilic E, Doeppner TR. CCL11 Differentially Affects Post-Stroke Brain Injury and Neuroregeneration in Mice Depending on Age. Cells. 2019 Dec 26;9(1):66. doi: 10.3390/cells9010066. PMID: 31888056; PMCID: PMC7017112.

34. Roy-O'Reilly M, Ritzel RM, Conway SE, Staff I, Fortunato G, McCullough LD. CCL11 (Eotaxin-1) Levels Predict Long-Term Functional Outcomes in Patients Following Ischemic Stroke. Transl Stroke Res. 2017 Dec;8(6):578-584. doi: 10.1007/s12975-017-0545-3. Epub 2017 Jun 21. PMID: 28634890; PMCID: PMC5648599.

35. Yu M, Ma X, Jiang D, Wang L, Zhan Q, Zhao J. CXC chemokine ligand 5 (CXCL5) disrupted the permeability of human brain microvascular endothelial cells via regulating p38 signal. Microbiol Immunol. 2021 Jan;65(1):40-47. doi: 10.1111/1348-0421.12854. Epub 2021 Jan 7. PMID: 33026667.